PONTIFICIA UNIVERSIDAD CATÓLICA DEL ECUADOR
FACULTAD DE CIENCIAS EXACTAS Y NATURALES
ESCUELA DE CIENCIAS BIOLÓGICAS

Systematics of *Pristimantis lacrimosus* group (Anura, Strabomantidae) with the description of a new species from the eastern slopes of the Ecuadorian Andes.

Disertación previa a la obtención del título de Licenciado en Ciencias Biológicas

JULIO CÉSAR CARRIÓN OLMEDO

Quito, 2020

Certifico que la disertación de Licencatura en Ciencias Biológicas del Sr. Julio César Carrión ha sido concluida en conformidad con las normas establecidas; por lo tanto, puede ser presentada para la calificación correspondiente

Santiago R. Ron, Ph. D
Director de la disertación

Quito, 27 de mayo de 2020

A los Pristimantis

INDEX

LIST OF TABLES……VII

LIST OF FIGURES ……VIII

MANUSCRIPT……10

Abstract ……..10

1. Introduction ……10

2. Materials and methods…….....12

2.1. *Nomenclature*……..12

2.2. *DNA extraction, amplification and sequencing*……..12

2.3. *Phylogeny*……13

2.4. Morphology…….13

2.5. Bioacoustics……14

3. Results ...……...15

3.1. *Phylogeny and genetic distances*……..…….15

3.2. *Morphometric analyses* ……..16

4. Systematics……16

5. *Pristimantis lacrimosus* group……..16

5.1. *Content*……16

5.2. *Distribution*……..…..….16

5.3. *Remarks*……..17

6. *Pristimantis petersioides* sp.nov. ……..….17

6.1. *Holotype* ……17

6.2. *Paratypes*……..…...17

6.3. *Diagnosis*……18

6.4. *Comparison with other species*…..…….……...18

6.5. *Description of the Holotype*……19

6.6. *Variation*…..…….…….20

6.7. *Variation in life*..……...…….…..….21

6.8. *Advertisement call*…….….21

6.9. *Distribution and natural history*……..…..……..21

6.10. *Etymology*……21

6.11. *Conservation status*…….…..…21

6.12. *Remarks*…….…..….22

7. Discussion……22
7.1. *On the identity of Pristimantis petersi*……22
7.2. *Use of bioacoustics for species delimitation* ……23
8. Acknowledgements……..24
9. Literature cited……24
10. Tables……29
11. Figures……..36

LIST OF TABLES

Table 1. Genbank accession numbers for DNA sequences used for phylogenetic analyses.……..…….....……29

Table 2. Character loadings, eigenvalues, and percentage of explained variance for Principal Components (PC) I–II. …….…..…...32

Table 3. Quantitative and qualitative characteristics of the advertisement call of *Pristimantis petersioides* sp. nov.…….……..…..33

Table 4. Qualitative morphological characters of species most similar to *Pristimantis petersioides* sp. nov.…….…….34

Table 5. Morphometric variables of *P. petersioides* sp. nov. and *P. petersi*….....35

LIST OF FIGURES

Figure 1. Maximum likelihood tree showing the sister clades of *Pristimantis lacrimosus* group …….…….....36

Figure 2. Principal components 1 and 2 from analysis of five size-corrected morphological variables. See Table 2 for character loadings on each component.….38

Figure 3. Holotype of *Pristimantis petersioides.* QCAZ 58939, adult female, SVL = 22.02 mm.…… …….…..39

Figure 4. Hand and foot of the holotype of *Pristimantis petersioides* sp. nov…..…..40

Figure 5 Live specimens of *Pristimantis petersioides* sp. nov. and most similar species……..……41

Figure 6. Color variation in preserved individuals of *Pristimantis petersioides* ...…42

Figure 7. Variation in live adult individuals of *Pristimantis petersioides*.…….43

Figure 8. Oscillogram (A) and sound spectrogram (B) of a call series of *Pristimantis petersioides* sp. nov……..…….……..44

Figure 9. Oscillogram (top), sound spectrogram (middle), and power spectrum (bottom) of advertisement calls of *Pristimantis petersioides* sp. nov…….45

Figure 10. Records of *Pristimantis petersioides* sp. nov., *Pristimantis petersi*, *Pristimantis* sp. UCS1, *Pristimantis* sp. UCS2, *Pristimantis* sp. UCS3…….46

Figure 11. Variation in live adult individuals of *Pristimantis petersi*……47

El presente trabajo se presenta en el formato de la revista ZooKeys a partir de la siguiente página.

Systematics of *Pristimantis lacrimosus* group (Anura, Strabomantidae) with the description of a new species from the eastern slopes of the Ecuadorian Andes

Julio C. Carrión-Olmedo[1] and Santiago R. Ron[1]

[1]*Museo de Zoología, Escuela de Ciencias Biológicas, Pontificia Universidad Católica del Ecuador, Av. 12 de Octubre y Roca, Aptdo. 17-01-2184, Quito, Ecuador*

Corresponding author: Santiago R. Ron (santiago.r.ron@gmail.com)

Abstract

With 540 species, the neotropical genus *Pristimantis* is the most speciose vertebrate genus. As a result of its striking diversity, taxonomic reviews remain a challenge. Herein, we present an updated phylogeny of the *Pristimantis lacrimosus* group, report the presence of three unconfirmed candidate species, and describe a new species from Llanganates and Sangay National Parks. Our phylogeny includes for the first time samples of *Pristimantis degener, P. eremitus, P. eugeniae, P. katoptroides and P. petersi.* Based on our phylogeny, we add 6 species to the *Pristimantis lacrimosus* group. Through the integration of molecular, morphologic, and bioacoustic evidence, we describe a new species which was hidden under "*Pristimantis petersi*". *Pristimantis petersioides* **sp. nov.** is most closely related to *Pristimantis petersi* and can be distinguished by its advertisement call, the presence of a discoidal fold and a snout rounded to truncate in dorsal view. *Pristimantis petersi* lacks discoidal fold and its dorsal snout shape is rounded. We suggest assigning the new species to the Endangered Red List category.

Keywords: Andes, Bioacoustics, Diversity, Phylogeny, *Pristimantis lacrimosus* group, Taxonomy.

Introduction

The genus *Pristimantis* has bewildered scientists for its striking diversity. Comprising 540 Neotropical species it is the most diverse vertebrate genus (Hedges et al. 2008, Frost 2019). In Ecuador, this genus represents more than one third of all anuran species, with 225 out of 629 species (Ron et al. 2019).

This astounding richness has been attributed to evolutionary innovations such as terrestrial breeding – direct embryonic development without a tadpole stage (Padial et al. 2014) – in synchronicity to the appearance of geographic barriers and great adaptability to occupy ecological niches not requiring aquatic environments for reproduction (Lynch and Duellman 1997, Mendoza et al. 2015).

Taxonomy within this group have been problematic and unstable because most taxonomic work has been based in morphological traits (Lynch and Duellman 1997), which can be highly variable and homoplastic (e.g. Guayasamin et al. 2015, Páez and Ron 2019). Those approaches are often insufficient to assess limits among closely related species. Thus, the use of DNA sequences is necessary to achieve better informed taxonomic decisions. The use of genetic evidence has speed up species discovery with more than 40 species of *Pristimantis* (e.g. Ortega et al. 2015, Guayasamin et al. 2017, Páez and Ron 2019) described in Ecuador in the last five years. Nevertheless, taxonomic problems in *Pristimantis* are still pervasive and are still far from being fully resolved (Ron et al. 2019).

The case of *Pristimantis lacrimosus* group exemplifies perfectly how difficult it is to assess evolutionary relationships. Hedges et al. (2008) proposed it as monophyletic based on molecular data of only three species. However, more recent phylogenies that include more species showed that this group is not monophyletic (Padial et al. 2014, Rivera-Correa and Daza 2016). Rivera-Correa and Daza (2016) identified two non-sister clades within *Pristimantis lacrimosus* group, "clade A" endemic to Colombia and "clade B" composed by species from Central America, Ecuador and Peru and suggested *Pristimantis lacrimosus* group may not represent a natural group. González-Durán et al. (2017) created *Pristimantis boulengeri* group for the "clade A" of Rivera-Correa and Daza (2016) and hypothesized that "clade B" corresponds to the *P. lacrimosus* species group and contains 25 species, however, phylogenetic position of *P. lacrimosus* were not tested.

Finally, phylogenetic position of *Pristimantis lacrimosus* and evolutionary relationships of *Pristimantis lacrimosus* species group has been recently clarified and the species content has been updated to 31 species (Ron et al. in press), however, there is still incomplete genetic sampling of 14 species included in this group.

A species of unknown phylogenetic position is *Pristimantis petersi* (Lynch and Duellman 1980). Since its description, this species suffered several taxonomic changes. Lynch (1991) changed its name to *Eleutherodactylus petersorum* to avoid homonymy with a Mexican species with the same epithet, which now is known as *Eleutherodactylus nitidus* (Peters 1870). Additionally, Lynch (1996) created the name *Eleutherodactylus johnwrighti,* as an amend to the previous epithet *petersorum*. Afterwards, Frost (2009) applied Article 59.4 of the International Code of Zoological Nomenclature making *Eleutherodactylus jonhwrighti* and *Eleutherodactylus petersorum* invalid replacement names because the taxa in question are not congeneric and recovered the first epithet used for this species.

Pristimantis petersi has been usually assigned to the *P. lacrimosus* species group. Lynch and Duellman (1980) placed it in the *P. unistrigatus* group, *P. lacrimosus* assembly. Later, Lynch and Duellman (1997) placed it in the *unistrigatus* group, *martinicensis* series. Hedges et al. (2008) proposed this species as a member of the *Pristimantis lacrimosus* group and Padial et al. (2014) and Rivera-Correa and Daza (2016) followed this proposal but without including *Pristimantis petersi* in their phylogenies.

Pristimantis petersi holotype (KU 143508) is from 16.5 km NNE of Santa Rosa, Napo Province, however, most specimens used in the species description by Lynch and Duellman (1980) were from other populations including localities in central Andes of Colombia (Huila and Putumayo Departments), and central Ecuador (Napo and Pastaza provinces). As currently defined, *Pristimantis petersi* is considered to have a wide distribution from the central Andes of Colombia (Lynch and Duellman 1980, Mueses-Cisneros 2005, Stuart et al. 2008) to the eastern slopes of the Ecuadorian Andes, from Sucumbíos to Morona Santiago Provinces at altitudes ranging between 1400–2000 m a.s.l (Brito et al. 2017, Ron et al. 2019). Lynch and Duellman (1980) mentioned that *Pristimantis petersi* exhibits body size variation throughout its distribution range and, remarkably, realized that individuals from the upper Pastaza trench were larger than individuals from the type locality, Ecuador, and suspected that populations from Pastaza may represent another species.

This unusually large geographic distribution does not correspond to patterns observed in montane frogs (Wollenberg et al. 2008). In addition, reports of body size variation throughout populations (Lynch and Duellman 1980, Brito et al. 2017) suggest that *Pristimantis petersi*, as currently defined, might be a species complex. Guayasamin and Funk (2009) tentatively reported an abundant population of *Pristimantis* cf. *petersi* at Yanayacu Biological Station. Brito et al. (2017) reported an abundant species in the upper basin of the Upano river, Sangay National Park, Morona Santiago Province referred as "*Pristimantis petersi*" and also as "*P.* aff. *petersi*".

Recent fieldwork conducted by field staff of the QCAZ museum from Pontificia Universidad Católica del Ecuador resulted in collections of *P. petersi* near its type locality and in the discovery of populations of a species similar to *P. petersi* in Sangay National Park and Llanganates National Park. Through the integration of morphological, genetic, and bioacoustic data with an exhaustive population sampling we demonstrate that those populations are distinct from *P. petersi*. We describe the new species and review the content and phylogenetic relationships of the *Pristimantis lacrimosus* group.

Materials and Methods

Nomenclature

Generic names follow Duellman and Lehr (2009) and AmphibiaWeb (2019).

DNA extraction, amplification and sequencing

We inferred the phylogenetic relationships of the new species and closely related taxa based on DNA sequences of one nuclear gene: Recombination activating gene 1 (RAG-1) and three mitochondrial genes: 12S rRNA (12S), 16S rRNA (16S), NADH dehydrogenase subunit 1 (ND1) and their flanking tRNAs. DNA was extracted from muscle or liver tissue preserved in 95% ethanol using standard

Guanidine thiocyanate extraction protocols. We used polymerase chain reaction (PCR) to amplify DNA fragments. Primers used for amplification of 12S were t-Phe-frog and t-Val-frog (Wiens et al. 2005), 12SZ-L and 12SK-H (Goebel et al. 1999), for 16S, primers were 12sL13 (Feller and Hedges 1998), 16L19 and 16H36E (Heinicke et al. 2007), for ND1, primers were WL379, WL384, t-Met-frog and 16S-frog (Moen and Wiens 2009), for RAG1, primers were R182, R270, Rag1FF2, Rag1FR2 (Heinicke et al. 2007). PCR amplification was performed under standard protocols and sequenced in both directions by the Macrogen Sequencing Team (Macrogen Inc., Seoul, Korea). All sequences were assembled in Geneious 7.1.7., then exported to Mesquite version 3.40 where each genomic region was aligned separately using default parameters in Muscle (Edgar 2004). Unambiguous alignment errors were corrected manually in Mesquite (Maddison and Maddison 2018). The aligned matrix is available in https://zenodo.org/ under doi:10.5281/zenodo.3785738. To calculate the uncorrected p distances of 16S we used MEGA7 on a fragment of 653 pb (Kumar et al. 2016).

We included 152 available GenBank sequences of congeneric species. To find sequences in GenBank, we made a 16S BLASTn search with the sequences of *Pristimantis petersioides* sp. nov. (Table 1). These searches showed that the most similar sequences belong to species from the *Pristimantis lacrimosus* group: *P. schultei* (identity 88.62%, accession EF493681), *P. bromeliaceus* (identity 86.92%, accession EF493351.1) and others such as *P. galdi* (identity 87.76%, accession EU186670.1), and *P.* cf. *mendax* (identity 87.07%, accession EU186659.1). Therefore, we included sequences used in previous studies on *Pristimantis lacrimosus* group (e.g. Arteaga et al. 2013, Padial et al. 2014, Ortega-Andrade et al. 2015, Rivera-Correa and Daza 2016, Guayasamin et al. 2017, Ron et al. in press). Samples of *Niceforonia nigrovittata, N. elassodisca*, and *Pristimantis w-nigrum* were set as outgroups. The combined DNA matrix had up to 4021 bp and 118 terminals.

Phylogeny

The phylogeny was inferred using Maximum Likelihood as optimality criterion. To choose the substitution models that best adjusted to our sequences, we used Model Finder under the command MFP+MERGE (Kalyaanamoorthy et al. 2017, Chernomor et al. 2016) as implemented in IQ-TREE 1.6.8 (Nguyen et al. 2015). We partitioned the sequences by gene and by codon position in coding genes. For the ML search we used IQ-TREE 1.6.8 (Nguyen et al. 2015) under default values. To assess branch support we made non-parametric bootstraps with 200 pseudoreplicates (command -b in IQ-TREE). Additionally, we inferred phylogenies from mithocondrial DNA and nuclear gene RAG1 separately to compare the topology of the phylogenetic tree derived from DNA regions with independent segregation.

Morphology

Diagnostic characters and comparisons are based on specimens from Museo de Zoología at Pontificia Universidad Católica del Ecuador, Quito (QCAZ). Examined specimens are listed as Supplementary File 1. Character definitions and terminology follow Duellman and Lehr (2009). Sex was determined by presence of nuptial pads or vocal slits, and direct inspection of gonads. Descriptions of coloration in life are based

on digital photographs. We examined the following qualitative characters: dorsal and ventral skin texture, presence of tympanic membrane and annulus, snout shape, presence of rostral papilla, presence of vomerine odontophores, presence of vocal slit and gular sac in males, relative length of fingers and toes, disc shape, presence of dorsolateral, discoidal and supratympanic folds, presence of lateral fringes on fingers and toes, presence of palmar, ulnar, tarsal, metatarsal, subarticular, supernumerary, knee, heel, and eyelid tubercles, and webbing on fingers and toes. We follow the name "hyperdistal tubercle" proposed in Ospina-Sarria and Duellman (2019) to refer to the most distal tubercle in Finger III and in Toe IV.

Adults were measured with digital calipers (to the nearest ±0.01mm) for eleven morphological variables, following Duellman and Lehr (2009): (1) snout-vent length; (2) tibia length; (3) foot length; (4) head length; (5) head width; (6) eye diameter; (7) tympanum diameter; (8) interorbital distance; (9) eye width; (10) internarial distance; (11) eye-nostril distance. Morphometric analyses were performed based on measurements of adults (number of specimens in parenthesis): *P. petersi* (12), *P. petersioides* sp. nov. (54).

We carry out linear regressions to adjust morphological variables to difference in body size to isolate changes in allometry. We obtained residuals from tibia length, foot length, head width, head length and tympanum with snout-vent length (SVL). We ran a MANOVA to test the presence of sexual dimorphism on both species using regression residuals. Morphometric variables associated with eyes (i.e., eye diameter, interorbital distance, eyelid width, internarial distance and eye-nostril distance) had weak correlation with snout-vent length. Low correlation appears to be a result of the difficulty of defining the eye edge on preserved specimens. Therefore, were removed those variables from the analysis. To explore morphometric differentiation between species, we applied a Principal Components Analysis using the SVL residuals.

Bioacoustics

We analyzed calls from three adult males of *Pristimantis petersioides* sp. nov., one individual (not collected) from Sardinayacu, Sangay National Park, Morona Santiago Province, recorded by Diego Batallas; QCAZ 58940 from Refuge 1, Sardinayacu, Sangay National Park, Morona Santiago Province (2.0983° S, 78.1555° W, 1406 m a.s.l) collected on 21 January 2015, air temperature 19 ºC, recorded in situ by Daniel Rivadeneira, and QCAZ 59466 from the ravines of Yurugyacu river, Llanganates National Park, Pastaza Province, (1.3524º S, 78.0597º W, 1419 m a.s.l.) collected on February 24 2015 and recorded in captivity on 6 March 2015 by Santiago R. Ron. Advertisement calls of *Pristimantis petersi* were analyzed from two adult males (not collected) from near its type locality, Cocodrilos, Napo Province, (0.66812° S, 77.7975° W, 1725 m a.s.l) recorded on 22 June 2016 by Santiago R. Ron. Recordings were made in WAV format, with a sample rate of 44100 Hz and 16-bits. Call variables were measured with RAVEN PRO 1.5 (Charif et al. 2010), under a Hanning function, 2048 DFT, sample rate of 46 kHz and a grid spacing of 20 kHz.

We followed the call-centered approach (*sensu* Köhler et al. 2017) for call measurements and terminology. Eight acoustic parameters (modified from Köhler et al. 2017) were measured: (1) Call duration = time from beginning to end of one call,

measured from oscillogram; (2) Call rate = number of calls per minute; (3) Call interval = time from end of call to beginning of next call;(4) Call rise time = time from beginning of call to point of maximum amplitude; (5) Amplitude modulation = change in the amplitude level of a sound wave over time; (6) Frequency band = difference between upper and lower frequencies measured along entire call (7) Fundamental frequency = frequency with highest energy on 1st harmonic in the call; (8) Dominant frequency = frequency with highest energy along entire call. Recordings are deposited in the Sound Archive of Museo de Zoología QCAZ of Pontificia Universidad Católica del Ecuador (available at the Anfibios del Ecuador website, https://bioweb.bio/faunaweb/amphibiaweb/).

Results

Phylogeny and genetic distances

The best-fit models of DNA evolution, according to the BIC criterion, were TN+F+G4 for RAG1 first codon position, TPM3+F+R2 for RAG1 second codon position, K2P+G4 for RAG1 third codon position, GTR+F+I+G4 for 12S, TIM2+F+R5 for 16S, TIM2e+I+G4 for ND1 first codon position, TPM3+F+I+G4 for ND1 second codon position and TN+F+I+G4 for ND1 third codon position. The ML tree from mitochondrial DNA shows similar topology to the ML concatenated tree.

The Maximum Likelihood tree (Fig. 1) is similar in topology to Rivera-Correa and Daza (2016) and Ron et al. (in press). Support values for the *Pristimantis lacrimosus* group is strong (bootstrap = 97); this clade includes the species reported in Ron et al. (in press) as well as species not included in previous phylogenies as *P. degener, P. eremitus, P. petersi*, and *P. petersioides* sp. nov. Additionally, we report for the first time the phylogenetic position of *Pristimantis eugeniae* and *P. katoptroides. Pristimantis eugeniae* is the sister species of a clade formed by *P. glandulosus, P. acerus,* and *P. inusitatus* (bootstrap = 68). *Pristimantis katoptroides* is sister to (*P. quaquaversus*, *P. melanogaster)*. We also found that individuals identified as *Pristimantis subsigillatus* does not form a clade which suggests a thorough taxonomic revision is necessary. Individuals "*Pristimantis subsigillatus*" QCAZ 49637 and KU 218147 form the sister clade of *P. nyctophylax* (bootstrap = 100) and the remaining individuals identified as *Pristimantis subsigillatus* form a sister clade of *P. degener* (bootstrap = 100).

Pristimantis petersioides sp. nov. is the sister species of *P. petersi.* The uncorrected *p* genetic distances for 16S between *P. petersi* and *P. petersioides* sp. nov. range from 7.9% to 8.4%. Both species are sister to a candidate species from Bombuscaro, Podocarpus National Park, Zamora Province. Samples of *Pristimantis petersioides* sp. nov. separate in two sister clades, one restricted to Sardinayacu, Morona Santiago Province and the other to Zarentza, Pastaza Province; the uncorrected *p* genetic distances between these clades range from 1.2% to 1.4%.

The mtDNA tree shows strong support values for *Pristimantis lacrimosus* group (bootstrap = 99), for *Pristimantis petersi* (bootstrap = 100) and for *P. petersioides* sp. nov. (bootstrap = 99). The ML tree inferred from RAG1 shows lower support values

but is congruent in showing a monophyletic *Pristimantis lacrimosus* group (bootstrap = 96) and in confirming a close relationship between *P. petersi* and *P. petersioides* sp. nov. The mtDNA and RAG1 phylogenies do not show strongly supported incongruences. Mitochondrial DNA and RAG1 phylogenetic trees are available as Supplementary File 2.

Morphometric analysis

MANOVA results showed no sexual dimorphism on *Pristimantis petersioides* sp. nov. and *P. petersi*. The PCA show broad overlap in morphometric space between both species (Fig. 2). PC I had high loadings on head width, head length, and tibia length while PC II had a high loading on tympanum diameter. Both principal components explained 76.7 % of the morphometric variation (Table 2).

Systematic Account

The differences in morphology, advertisement calls, the branch lengths in the phylogeny, and genetic distances indicate that *Pristimantis petersioides* sp. nov. represents a different species from *P. petersi* (see below). In the following section, we update the species content for the *Pristimantis lacrimosus* group and describe the new species.

***Pristimantis lacrimosus* species group**

Content. We include all the descendants from the most recent common ancestor of *P. mindo* and *P. lacrimosus.* According to our findings and Ron et al. in press, the *Pristimantis lacrimosus* group comprises 37 species: *P. acuminatus* (Shreve, 1935), *P. amaguanae* Ron et al, in press, *P. aureolineatus* (Guayasamin, Ron, Cisneros-Heredia, Lamar and McCracken, 2006), *P. bromeliaceus* (Lynch, 1979), *P. crucifer* (Boulenger, 1899), *P. degener* (Lynch and Duellman, 1997), *P. ecuadorensis* Guayasamin et al, 2017, *P. enigmaticus* Ortega-Andrade et al, 2015, *P. eremitus* (Lynch ,1980), *P. galdi* Jiménez de la Espada, 1870, *P. geyi* Lehr, Gregory and Catenazzi, 2013, *P. jorgevelosai* (Lynch, 1994), *P. lacrimosus* (Jiménez de la Espada, 1875), *P. latericius* Batallas and Brito, 2014, *P. limoncochensis* Ortega-Andrade et al, 2015, *P. mendax* (Duellman, 1978), *P. mindo* Arteaga, Yanez-Munoz and Guayasamin, 2013, *P. moro* (Savage, 1965), *P. nankints* Ron et al, in press, *P. nyctophylax* (Lynch ,1976), *P. olivaceus* (Köhler, Morales, Lötters, Reichle and Aparicio, 1998), *P. omeviridis* Ortega-Andrade et al, 2015, *P. ornatissimus* (Despax, 1911), *P. padiali* Moravec, Lehr, Pérez-Peña, López, Gagliardi-Urrutia and Arista-Tuanama, 2010, *P. pardalinus* (Lehr, Lundberg, Aguilar and von May, 2006), *P. petersi* (Lynch and Duellman, 1980), *P. petersioides* sp. nov. (herein), *P. pseudoacuminatus* (Shreve, 1935), *P. romeroae* Ron et al, in press, *P. royi* (Morales, 2007), *P. schultei* (Duellman, 1990), *P. subsigillatus* (Boulenger, 1902), *P. tantanti* (Lehr, Torres-Gastello and Suárez-Segovia, 2007), *P. tayrona* (Lynch and Ruiz-Carranza, 1985), *P. waoranii* (McCracken, Forstner and Dixon, 2007), *P. zeuctotylus* (Lynch and Hoogmoed, 1977), and *P. zimmermanae* (Heyer and Hardy, 1991).

Distribution. The *Pristimantis lacrimosus* group is distributed in Central America, the Guianan Shield, northwestern Andes of Colombia (*P. jorgevelosai*), Pacific Basin of Ecuador, and the Amazon Basin. Its species richness peaks in the Ecuadorian Andes (n = 19) and Amazon basin of Ecuador and Peru (n = 14).

Remarks. We refrain from assigning *Pristimantis calima and Pristimantis sneiderni* (Ospina-Sarria and Duellman 2019) to the *Pristimantis lacrimosus* group due to the lack of molecular evidence, despite of the presence of hyperdistal tubercles and being morphologically similar to species of this group as *Pristimantis eugeniae, P. nyctophylax*, *P. subsigillatus*, and *P. schultei*.

***Pristimantis petersioides* sp. nov.**

Eleutherodactylus petersi Lynch and Duellman 1980 (in part)
Pristimantis petersi Batallas and Brito 2016
Pristimantis petersi Brito et al. 2017

Holotype. (Figs 3, 4) QCAZ 58939, adult female from Ecuador, Morona Santiago Province, Sangay National Park, Sardinayacu (2.09830° S, 78.15554° W), 1406 m a.s.l. Found in amplexus with QCAZ 58940. collected by D. Rivadeneira and Santiago R. Ron on 21 January 2015.

Paratypes (58: 39 adult males, 15 adult females, 4 juveniles). All individuals are adults unless otherwise noticed. All from Ecuador. *Napo Province*: QCAZ 46159, male, from Salcedo-Tena highway, Km 60 (0.9847º S, 78.1928 ºW, 2253 m a.s.l.), collected by Elicio Tapia and Fernando Nuñez in November 2009. *Morona Santiago Province*: Sangay National Park: QCAZ 58871, female, QCAZ 58944, male from Río Volcán (2.1008º S, 78.1559º W, 1345 m a.s.l.), collected by Daniel Rivadeneira, David Velalcázar, Javier Pinto, Francy Mora, Darwin Nuñez, Juan Carlos Sanchez, and Andrea Correa; QCAZ 58936, QCAZ 58939, QCAZ 58941, females, QCAZ 58940, QCAZ 58942–43, males from Refuge 1 (2.0988º S, 78.1561º W, 1406 m a.s.l.), QCAZ 58937–38, males from Chimerella lagoon (2.0885º S, 78.2069º W, 1650 m a.s.l.) collected by Daniel Rivadeneira, Francy Mora, Juan Carlos Sánchez and Andrea Correa; QCAZ 58881, QCAZ 58950, females, QCAZ 58949 male from the proximities of Cormorant lagoon (2.0738º S, 78.2195º W, 1835 m a.s.l.) collected by Javier Pinto, David Velalcázar and Darwin Nuñez, QCAZ 58880, QCAZ 58951, males from El Enmascarado lagoon (2.0600º S, 78.2207º W, 1796 m a.s.l.) collected by Javier Pinto, David Velalcázar and Darwin Nuñez. in January 2015. QCAZ 59166, female, QCAZ 59167, QCAZ58945–48, males from Refuge 3 (2.0757º S, 78.2157º W, 1724 m a.s.l.), collected by Santiago R. Ron, Diego Paucar, Pablo Venegas, Pamela Baldeón, Marcel Caminer and Kunam Nucirquia,; QCAZ 59169–71, males from Cormorant lagoon (2.0738º S, 78.2195º W, 1835 m a.s.l.), collected by Santiago R. Ron, Diego Paucar, Pablo Venegas, Pamela Baldeón, Marcel Caminer and Kunam Nucirquia, in February 2015. *Pastaza Province*: QCAZ 53227, female, from Anzu river (1.4177º S, 78.0485º W, 1272 m a.s.l), collected by Mauricio Ortega in May 2012. Llanganates National Park: QCAZ 45846–50, 45892, 45898, males, from Challuwa Yacu river, Ankaku Reserve (1.2792ºS, 78.0779º W, 2300 m a.s.l.) collected by Elicio Tapia and Silvia Aldás in October 2009; QCAZ 66553, male, from Ankaku Reserve (1.2770ºS, 78.0698ºW, 2216 m a.s.l.) collected by Diego Almeida,

Santiago Guamán, Darwin Nuñez, María José Navarrete, Verónica Andrade, Angel Alvarado, Fernando Alvarado in January 2017, QCAZ 59625, male, from Nuchimingue river (1.3626º S, 78.0582º W, 1350 m a.s.l.); QCAZ 59456, male, from Yurugyacu river (1.3560º S, 78.0592º W, 1354 m a.s.l.); QCAZ 59451, QCAZ 59467– 68, QCAZ 59479, males, from Zarentza community (1.3556º S, 78.0597º W, 1363 m a.s.l.); QCAZ 59458–59, females from near Yurugyacu river (1.3527º S, 78.0596ºW, 1354 m a.s.l.); QCAZ 59457, QCAZ 59465 females, QCAZ 59454–55, QCAZ 59462–63, QCAZ 59466, males, QCAZ59452–53, QCAZ59460, QCAZ59464, juveniles from the ravines of Yurugyacu river (1.3523º S, 78.0597º W, 1419 m a.s.l.); QCAZ 59470, QCAZ59472, females, QCAZ 59471, QCAZ 59473, males from Gustavo Ushpa house trail to Yurugyacu river (1.3430º S, 78.0574º W, 1221 m a.s.l.); QCAZ 59461, female, from La paila waterfall (1.3397º S, 78.0594º W, 1360 m a.s.l.) collected by Daniel Rivadeneira, Francy Mora, Juan Carlos Sánchez, David Velalcázar, Darwin Nuñez and Javier Pinto in February 2015.

Diagnosis. The assignment of the new species to the genus *Pristimantis* is based on the phylogeny (Fig. 1). *Pristimantis petersioides* is characterized by the following combination of characters: (1) Skin on dorsum smooth to shagreen with or without scattered small tubercles, head with or without one interorbital small tubercle, skin of venter weakly areolate; discoidal fold present, ill-defined; dorsolateral folds absent; (2) tympanic membrane and tympanic annulus present, round, its length 2/5 to 1/2 of eye diameter; its upper border weakly concealed by inconspicuous supratympanic fold; (3) snout rounded to truncate in dorsal view, truncate in lateral view, bearing a small rostral papilla; (4) interorbital space flat, broader than upper eyelid; upper eyelid with one distinct conical tubercle surrounded by lower, indistinct rounded tubercles; cranial crests absent; (5) vomerine odontophores low to prominent, oblique, moderately separated; posteromedial to choanae; (6) males with prominent, subgular vocal sac and vocal slits; (7) first finger shorter than second; all fingers long, discs broadly expanded, rounded to truncate; Finger III bearing a hyperdistal tubercle (Fig 4B) (8) fingers with narrow lateral fringes; (9) two ulnar tubercles; (10) no knee and heel tubercles, inner tarsal fold bearing 1–2 indistinct tubercles; (11) two metatarsal tubercles, inner oval, 3 times the size of outer conical to elliptical metatarsal tubercle; supernumerary plantar tubercles numerous; (12) toes with narrow lateral fringes; basal toe webbing absent, discs broadly expanded, Toe IV bearing an extra subarticular tubercle close to the disc referred as hyperdistal, Toe IV much larger than Toe III (disc on Toe III reaches proximal edge of penultimate subarticular tubercle on Toe IV, disc on Toe V exceeds the distal edge of penultimate subarticular tubercle on Toe IV), discs as expanded as those on fingers (Fig. 4A); (13) dorsum from dark olive green, orange brown to pale cream in life, with or without brown interorbital bar; face marks present as canthal and supratympanic stripes, and labial mark formed by indistinct dark brown dots; dorsum with scattered dark brown flecks, bearing irregular chevrons forming a triangle that extends from the ilium to the scapula, others with distinct dark brown dorsolateral stripes suffused with the supratympanic stripes; posterior half of flanks with dark browns flecks; venter pale creamy white; throat pale creamy white to pale brown; posterior surfaces of thighs pale cream to dark brown; iris reddish coppery with fine, dense, black reticulation ; (14) SVL 22.80 ± 1.37 mm (20.42–24.81 mm; n = 15) in females, 18.53 ± 1.52 mm (15.79–23.93 mm; n = 39) in males.

Comparison with other species. (coloration comparison based on digital photos of live specimens, otherwise noted) *Pristimantis petersioides* is most similar to other species of the *P. lacrimosus* group, especially *P. petersi* (Lynch and Duellman, 1980)*, P. bromeliaceus* (Lynch, 1979)*, P. lacrimosus* (Jiménez de la Espada, 1875) *, P. pastazensis* (Andersson, 1945), and *P. schultei* (Duellman, 1990) (Fig. 5). The uncorrected *p* genetic distances for gene 16S between individuals of *P. petersioides* and *P. petersi* range from 7.9% to 8.4%. Morphologically, *P. petersioides* can only be distinguished from *P. petersi* by the presence of a discoidal fold (absent in *P. petersi*). Additionally, its advertisement calls show significant differences in call duration and dominant frequency (Table 3). Call duration is shorter in *P. petersioides* 0.25 s (0.19–0.32 s; n = 3) than in *P. petersi*, 0.42 s (0.37–0.46 s; n = 2). Dominant frequencies also differ, while advertisement call of *P. petersioides* is 4430.79 Hz (4122–4837.22 Hz; n = 3), in *P. petersi* is 3956.75 Hz (3836.67–4076.84 Hz; n = 2). *Pristimantis petersioides* can be distinguished from *P. bromeliaceus* by snout shape (rounded to truncate in *P. petersioides* vs. subacuminate in *P. bromeliaceus*), texture of ventral skin (weakly areolate in *P. petersioides* vs. coarsely areolate in *P. bromeliaceus*), iris coloration (reddish coppery in *P. petersioides* vs. brown flecked with gold or bronze in *P. bromeliaceus*), and by having an eyelid with one conical tubercle surrounded by lower tubercles (two to three non-conical tubercles in *P. bromeliaceus*). *Pristimantis petersioides* differs from *P. lacrimosus* (Jimenez de la Espada 1875) in dorsal coloration (dark greenish brown to pale yellowish green in *P. petersioides* vs. golden brown in *P. lacrimosus*), presence of eyelid tubercles and narrow lateral fringes (both absent in *P. lacrimosus*), and size of outer metatarsal tubercle (3x bigger than the inner metatarsal tubercle in *P. petersioides* vs. 5–6x bigger in *P. lacrimosus*). *Pristimantis petersioides* is also similar to *P. rhodostichus* and *P. schultei* from Peru and Ecuador. It can be distinguished from both by the snout shape in dorsal view (rounded to truncate in *P. petersioides* vs. long acuminate in *P. rhodostichus* and acuminate in *P. schultei*). It can be further distinguished from *P. schultei* by lacking heel tubercles (present in *P. schultei*), and from *P. rhodostichus* by lacking red markings on the dorsum (present in *P. rhodostichus*). Additionally, *P. petersioides* differs from *P. pastazensis* (Andersson 1945) by snout shape in dorsal view (rounded to truncate in *P. petersioides vs.* subacuminate in *P. pastazensis*) and in lateral view (truncate in *P. petersioides vs.* protruding in *P. pastazensis*), tubercles on upper eyelid (one distinct conical tubercle surrounded by lower, indistinct rounded tubercles in *P. petersioides* vs. several scattered, low subconical tubercles), and skin of venter (weakly areolate in *P. petersioides* vs. coarsely areolate in *P. pastazensis*).

Description of the holotype. Adult female (QCAZ 58939). Measurements (in mm): SVL 22.02; tibia length 12.07; foot length 10.72; head length 8.82; head width 9.09; eye diameter 2.96; tympanum diameter 1.35; interorbital distance 2.52; upper eyelid width 2.44; internarial distance 1.59; eye-nostril distance 2.59; tympanum-eye distance 0.71. Body slender; head slightly wider than long, wider than body; snout rounded to truncate with rostral papilla in dorsal view, truncate in lateral profile; canthus rostralis distinct, slightly curved in dorsal view; loreal region concave; interorbital space flat, no cranial crests; eye large, protuberant; upper eyelid about 97% of interorbital distance, bearing one subconical tubercle. Tympanic membrane and annulus distinct, rounded in shape, with inconspicuous supratympanic fold, partially obscuring anterodorsal edge; horizontal diameter of tympanum about 13% of head length, separated from eye by a distance about one half tympanum length; choanae large, rounded, not concealed by palatal shelf of maxillary arc; dentigerous

processes of vomers prominent, oblique, bearing a transverse row of five teeth; tongue big, elliptical, posterior border slightly notched, 40% of the anterior surface adherent to floor of mouth. Skin on dorsum smooth to shagreen; dorsolateral folds absent; skin on upper flanks bearing scattered low tubercles; skin on belly shagreened to weakly areolate; skin on throat and chest smooth; discoidal fold ill-defined; skin in upper cloacal region shagreen. Forearms slender bearing low antebrachial tubercle and one subconical ulnar tubercle at the distal half of the forearm; fingers large and slender, all with oval (broader than long) pads, all finger with discs; fingers bearing narrow lateral fringes; relative lengths of fingers I < II < IV < III; three subarticular tubercles on finger III (Fig. 4B), the most distal tubercle we refer as hyperdistal, all the tubercles well defined, round in ventral and lateral view; several supernumerary tubercles present, prominent at the base of the fingers and lower, indistinct at the palmar surface; palmar tubercle bifid, heart-shaped, about the same length and twice the width of elliptical thenar tubercle (Fig. 4B).

Hindlimbs slender; tibia length about 55% of SVL; upper surfaces of hindlimbs smooth; foot length about 48% of SVL, posterior surfaces of thighs smooth, ventral surfaces of thighs slightly areolate; knee and heel lacking tubercles; outer surface of tarsus bearing three low, inconspicuous tubercles, equally distributed along tarsus; toes bearing narrow lateral fringes; webbing between toes absent; discs on toes broadly expanded more than those on fingers, rounded; relative lengths of toes: I < II < III < V < IV; Toe V much longer than Toe III (disc on Toe III reaches proximal edge of penultimate subarticular tubercle on Toe IV, disc on Toe V exceeds the distal edge of penultimate subarticular tubercle on Toe IV), subarticular tubercles rounded, simple, elevated; plantar surface with low supernumerary tubercles, bearing four subarticular tubercles (Fig. 4A), inner metatarsal tubercle prominent, elliptical, approximately twice size of rounded, conical outer metatarsal tubercle (Fig. 4A).
Color of holotype in preservative. (Figs 3C, 3D) Background color pale grayish cream with scattered, irregular dark brown chevrons, head bearing dark drown supratympanic and canthal stripe, upper lip bearing ill-defined stripe formed by irregular dark brown dots; upper flanks bearing dark brown, irregular flecks and blotches densely distributed; venter, ventral surfaces of forearms and hindlimbs pale creamy white, chest and throat with diminutive dark brown dots uniformly distributed (visible under magnification); ventral surfaces of hands and foot with dense minute dark brown dots.
Color of holotype in life. (Figs 3A, 3B) Dorsal surfaces yellowish green with scattered, irregular dark brown chevrons; canthal stripe and supratympanic fold black, upper flanks pale cream with dark brown irregular flecks and blotches; venter creamy white; axils pinkish white; ventral surfaces of limbs, thighs yellowish green; iris reddish copper with dark bronze faint horizontal streak and thin irregular black reticulations.

Variation in preservative. (Fig. 6) Adult males (15.79–23.93 mm) are smaller than adult females (20.42–24.81 mm). See Table 5 for measurements of the type series. Males bearing vocal slits and prominent subgular sac, lacking nuptial pads. Dorsal background coloration in preserved specimens varies from uniform dark brown (e.g., QCAZ 59461, QCAZ 58951, QCAZ 59451) to pale cream (e.g., QCAZ 59166, QCAZ 58881, QCAZ 58936). Marks on dorsum varies from scattered, irregular dark brown chevrons that form a triangle extending from the ilium to the

scapula (e.g., QCAZ 58950, QCAZ 59468), ill-defined, dark brown flecks and spots (e.g., QCAZ 59472, QCAZ 58948), pale cream middorsal bar from the snout to the cloaca (e.g., QCAZ 59456), to black dorsolateral stripes suffused with supratympanic stripes (e.g., QCAZ 59171, QCAZ 58943), with or without dark interorbital bar.

Variation in life. (Fig. 7). Tuberculation pattern varies from dorsum completely smooth (e.g., QCAZ 58943, QCAZ 58951) to dorsum shagreen (e.g., QCAZ 58938, QCAZ 58939), some individuals bear scattered tubercles on anterior half of dorsum (e.g., QCAZ 58880) or have the dorsum densely tuberculated (e.g., QCAZ 59463). When dorsum is tuberculated, flanks and limbs usually bear scattered tubercles more conspicuous than those in the dorsum. Similarly, the interorbital tubercle and upper eyelid tubercles are more prominent when the dorsum is tuberculated. Dorsum varies from dark greenish brown (e.g., QCAZ 59471), bright orange (e.g., QCAZ 58943), olive green (e.g., QCAZ 58938), to pale yellowish green (e.g., QCAZ 58941). Dark marks on dorsum varies from scattered, irregular brown chevrons that form a triangle that extends from the ilium to the scapula, to ill-defined, dark brown flecks and spots (e.g., QCAZ 59455, QCAZ 58948). Some individuals bear bright orange blotches limited by dark brown contours (e.g., QCAZ 59458, QCAZ 58951), bright orange middorsal bar that extends from the snout to the cloaca (e.g., QCAZ 59456), black dorsolateral stripes suffused with supratympanic stripes (e.g., QCAZ 58943). Interorbital stripe or bar may be present in some individuals (e.g., QCAZ 59455, QCAZ 59458) or absent (e.g., QCAZ 58943, QCAZ 59456). Snout varies from dark greenish brown, pale yellowish green to bright orange (e.g., QCAZ 59471, QCAZ 59455, QCAZ 59466), some individuals bear a bright orange to yellow interorbital bar with a darker contour (e.g., QCAZ 58951, QCAZ 59462, QCAZ 59458).

Advertisement call. Quantitative measurements of the advertisement call of *Pristimantis petersioides* (QCAZ 58940) are shown in Table 3. The call is a click with an average duration of 0.25 s (0.19–0.32 s; n = 3; Fig. 8). The highest peak of the amplitude is at 20–30 ms and decreases gradually towards the end (Fig. 9). The calls are repeated at a mean rate of 19.89 calls per minute (11.26–25.78; n = 3). Three or four harmonics are present, but most of the energy is located at the first one. Dominant frequency is 4430.79 Hz (4122–4837.22 Hz; n = 3)

Distribution and natural history. *Pristimantis petersioides* is known from five localities in the eastern Andean slopes of central Ecuador between 1221–2300 m a.s.l. (Fig. 10). It inhabits the Eastern Andean Foothills Forest and Eastern Montane Forest natural regions (as defined by Ron et al. 2019). It has been recorded in primary forest and, less frequently, in secondary forest. Individuals were found during nocturnal surveys, usually perching on ferns, herbs, or *Heliconia* leaves, branches, or inside bromeliads up to 350 cm above the ground, usually near water bodies. Amplectant pairs were found on March 2015 in Sardinayacu and Zarentza.

Etymology. The specific epithet is a masculine noun in apposition. The suffix *oides* is derived from the Greek *eidos* meaning similar. The name makes reference to the similarity between the new species and its sister species, *Pristimantis petersi.*

Conservation status. Four out of five known localities are inside National Parks (Sardinayacu in Parque Nacional Sangay and Ankaku, Zarentza and Salcedo-

Tena highway in Parque Nacional Llanganates); nonetheless, based on a vegetation cover map (Ministerio del Ambiente 2018a) and a deforestation map 2016–2018 (Ministerio del Ambiente 2018b), Zarentza is < 1 km from deforested areas for agriculture. At the year of collection (2009) the locality at Salcedo-Tena highway was in a forested region with small deforested patches at distances > 2.5 km (based on a 2008 deforestation map by Ministerio de Ambiente). Sardinayacu, refuge 3 occur > 6 km from pastures, while Sardinayacu, refuge 1 is < 0.5 km from deforested areas for agriculture.

In Sardinayacu, this species was one of the most common during surveys (24 individuals found in 9 days by 13 people) which suggest it is locally abundant. Records of this species showed very clumped distribution in the proximities of Sardinayacu refuges, Sangay National Park and Zarentza community and Ankaku reserve , Llanganates National Park respectively. Its extent of occurrence is 1402 km^2 (based on a minimum convex polygon). We consider *Pristimantis petersioides* to be in the category Endangered (EN) following B1ab(iii) IUCN criteria because: (i) it is only known from five localities (sensu IUCN 2017), (ii) its Extent of Ocurrence is less than 5000 km^2 (1402 km^2); and approximately 9% of its Extent of Ocurrence has been affected by deforestation, human settlements and agriculture.

Remarks. *Pristimantis petersioides* differs from *P.* sp. UCS1 (QCAZ 60398) by the snout shape (dorsally rounded in *P. petersioides,* dorsally subacuminate in *P.* sp. UCS1), venter texture (weakly areolate in *P. petersioides;* coarsely areolate in *P.* sp. UCS1), presence of small rostral papilla (absent in *P.* sp. UCS1); furthermore, *P. petersioides* bears a complete, rounded tympanic annulus, weakly obscured posterodorsally by a thin supratympanic fold (tympanic annulus concealed posterodorsally by a thick supratympanic fold in *P.* sp. n. UCS1). It also differs from *P.* sp. UCS2 (QCAZ62940) by the presence of a small rostral papilla (*P.* sp. UCS2 lacks rostral papilla), moreover, dorsal coloration is creamy orange in *P.* sp. UCS2 while *P. petersioides* varies from dark greenish brown to pale yellowish green. *Pristimantis petersioides* differs from *P.* sp. UCS3 (QCAZ 58956) by snout shape in dorsal view (rounded to truncate in *P. petersioides* vs. acuminate in *P. bromeliaceus*), texture of ventral skin (weakly areolate in *P. petersioides* vs. coarsely areolate in *P.*sp. UCS3), and by the presence of small rostral papilla (absent in *P.* sp. UCS3).

Discussion

On the identity of Pristimantis petersi

Pristimantis petersi was considered to have a wide distribution from the central Andes of Colombia in Caquetá, Huila, and Putumayo (Lynch and Duellman 1980, Mueses-Cisneros 2005, Stuart et al. 2008), to the eastern slopes of the Ecuadorian Andes, from Sucumbíos to Morona Santiago Provinces (Brito et al. 2017, Ron et al. 2019). Herein, we show that it was composed of two species which appear to be allopatric, south and north of the Quilindaña paramos in Napo Province.
Lynch and Duellman (1980) remark of size differences between populations of from the north (*P. petersi*) and south (*P. petersioides*) was not supported in our data but their suspicion of the distinctiveness of the populations from the Pastaza trench was correct. Based in our review, we tentatively consider *Pristimantis petersi* as

distributed from the central Andes of Colombia to Napo Province (Fig. 10). We recommend to examine the identity of Colombian populations using genetic data. Recent reviews of Andean *Pristimantis* indicate that species usually have a restricted distribution (e.g., Páez and Ron 2019). The geographic distance of Colombian populations (up to 320 km from the type locality) suggest that, at least some of them, could represent a separate species.

Our results show that eastern montane forests still harbor a large number of undescribed species of *Pristimantis.* Similar findings have been previously reported by Ortega et al. (2015), Páez and Ron (2019), and Ron et al. (in press). As in previous reviews (e.g., Restrepo et al. 2017, Páez and Ron 2019), we also found broad intraspecific and intrapopulation variation in dorsal color within *P. petersioides* (Figs. 6, 7) and *P. petersi* (Fig. 11). This large intraspecific and intrapopulation variation hinders the use of dorsal coloration for diagnosis between both species. Most individuals have greenish dorsal color which is characteristic of several species of the *P. lacrimosus* group. We found few diagnostic morphological characters to distinguish the new species from *Pristimantis petersi,* which highlights the importance of combining several character types in addition to morphology (e.g. molecular and bioacoustic) in order to clarify species identity.

Use of bioacoustics for species delimitation

Herein, we discover a confirmed candidate species (*sensu* Vieites et al. 2009), which we describe as *P. petersioides*, because of its high genetic differentiation, morphological distinctiveness and differences in advertisement calls. For the individuals reported by Ron et al (in press) as *Pristimantis* sp. QCAZ 60398, QCAZ 58956 and as *P. bromeliaceus* QCAZ 62940 we suggest the category of unconfirmed candidate species (*sensu* Vieites et al. 2009) because they show deep molecular divergence, but we lack additional data to confirm their status.

Our morphometric analysis was of little help to distinguish closely related species. In contrast, advertisement calls were essential to support the taxonomic identity of the new species as in previous studies (Caminer et al. 2014, Ron et al. 2018, Páez and Ron, 2019). Bioacoustics analyses are of importance for taxonomy because advertisement calls mediate species recognition (e.g., Ryan and Rand 1995). Differences in static characters (e.g., dominant frequency) suggest the existence of reproductive isolation between species (Köhler et al. 2017).

Despite of showing similarities in qualitative traits –a series of short calls with one single note– in both *Pristimantis petersi* and *P. petersioides*; we have found differences –little or no overlap in their range values– in the most relevant quantitative traits *sensu* Köhler et al. (2017) as call duration and dominant frequency.

Acknowledgements

This study was funded by the Secretaría de Educación Superior, Ciencia, Tecnología e Innovación del Ecuador SENESCYT, Arca de Noé Iniative and Pontificia Universidad Católica del Ecuador. We are thankful to QCAZ Molecular Laboratory, specially to Ana Belén Carrillo and Claudia Terán for their guidance during labwork. The staff of QCAZ museum, Fernando Ayala, Santiago Guamán and Diego Paucar helped with preservation and processing of the specimens. Diego Batallas provided a call recording from an individual from Sangay National Park. Daniel Rivadeneira made call recordings. Special thanks to Jhael Ortega and Yerka Sagredo for their assistance with specimen examination. Marcel Caminer, María José Navarrete and Jhael Ortega provided helpful observations and guidance during this research and constructive comments to previous versions of this manuscript. Alex Achig, Silvia Aldás, Ángel Alvarado, Fernando Alvarado, Verónica Andrade, Pamela Baldeón, Marcel Caminer, Andrea Correa, Santiago Guamán, María José Navarrete, Darwin Nuñez, Fernando Nuñez, Kunam Nucirquia,, Diego Paucar, Javier Pinto, Belén Proaño, Daniel Rivadeneira, Juan Carlos Sánchez, Elicio Tapia ,David Velalcázar, Pablo Venegas and Mario Yánez collected specimens. We thank Jorge Brito, Valeria Chasiluisa, Diego Paucar, Juan Carlos Sánchez and David Velalcázar for providing specimen photographs. The ecuadorian Ministerio del Ambiente provided research permits numbers 008-09 IC-FAU-DNB/MA, 001-11 IC-FAU-DNB/MA, 002-16 IC-FAU-DNB/MA and MAE-DNB-ARRGG-CM-2014-0002.

Literature Cited

Andersson LG (1945) Batrachians from East Ecuador collected 1937,1938 by Wm. Clarke-MacIntyre and Rolf Blomberg. Arkiv för Zoologi. Kongliga Svenska Vetenskaps-Akademiens, Stockholm. Arnoldia, Zimbabwe 37:32143.

AmphibiaWeb (2019) AmphibiaWeb: information on amphibian biology and conservation. http://amphibiaweb.org/. University of California Berkeley.

Batallas DR, Brito JM (2016) Análisis bioacústico de las vocalizaciones de seis especies de anuros de la laguna Cormorán, complejo lacustre de Sardinayacu, Parque Nacional Sangay, Ecuador. Revista Mexicana de Biodiversidad 87, 1292–1300.

Brito JM, Batallas D, and Yánez-Muñoz MH (2017). Ranas terrestres *Pristimantis* (Anura: Craugastoridae) de los bosques montanos del río Upano, Ecuador: Lista anotada, patrones de diversidad y descripción de cuatro especies nuevas . Neotropical Biodiversity, 3, 125–156. https://doi.org/10.1080/23766808.2017.1299529

Caminer MA, Ron SR (2014) Systematics of treefrogs of the *Hypsiboas calcaratus* and *Hypsiboas fasciatus* species complex (Anura, Hylidae) with the description of four new species. ZooKeys 370, 1–68. https://doi.org/10.3897/zookeys.370.6291

Charif RA, Waack AM, Strickman LM (2010) Raven Pro 1.4 User's Manual. Ithaca, NY, Cornell Lab of Ornithology.

Chernomor O, von Haeseler A, Minh BQ (2016) Terrace aware data structure for phylogenomic inference from supermatrices. Systematic Biology, 65, 997–1008. https://doi.org/10.1093/sysbio/syw037

646 Duellman WE, Lehr E (2009) Terrestrial-breeding frogs (Strabomantidae) in Peru.
647 Munster, Germany: Nature und Tier Verlag, 382 pp.

648 Duellman WE, Pramuk JB (1999) Frogs of the genus *Eleutherodactylus* (Anura:
649 Leptodactylidae) in the Andes of northern Peru. Scientific Papers. Natural History
650 Museum, University of Kansas 13, 1–78. https://doi.org/10.5962/bhl.title.16169

651 Duellman, W. E. 1990. A new species of *Eleutherodactylus* from the Andes of
652 northern Peru (Anura: Leptodactylidae). Journal of Herpetology 24, 348–350.

653 Edgar RC (2004) MUSCLE: multiple sequence alignment with high accuracy and
654 high throughput. Nucleic Acids Research, 32,1792–1797.

655 Feller AE, Hedges SB (1998). Molecular Evidence for the Early History of Living
656 Amphibians. Molecular Phylogenetics and Evolution, 9, 509–516.
657 doi:10.1006/mpev.1998.0500

658 Frost DR (2009). Amphibian Species of the World: An Online Reference. Version
659 5.3. (12 February 2009). Electronic Database. New York, USA: American Museum of
660 Natural History.

661 Frost DR (2019) Amphibian Species of the World: an Online Reference [Internet].
662 Version 6.0. New York (NY): American Museum of Natural
663 History;http://research.amnh.org/herpetology/amphibia/index.html, [accessed May 5
664 2019].

665 Goebel AM, Donnelly MA, Atz M (1999) PCR primers and amplification methods for
666 12S ribosomal DNA, the control region, cytochrome oxidase I, and cytochrome b in
667 bufonids and other frogs, and an overview of PCR rimers which have amplified DNA
668 in amphibians successfully. Molecular Phylogenetics and Evolution 11, 163–199.

669 González-Durán GA, Targino M, Rada M, Grant T (2017) Phylogenetic relationships
670 and morphology of the *Pristimantis leptolophus* species group (Amphibia: Anura:
671 Brachycephaloidea), with the recognition of a new species group in *Pristimantis*
672 Jiménez de la Espada, 1870. Zootaxa, 4243, 42–74.

673 Guayasamin JM, Funk WC (2009) The amphibian community at Yanayacu Biological
674 Station, Ecuador, with a comparison of vertical microhabitat use among *Pristimantis*
675 species and the description of a new species of the *Pristimantis myersi* group. Zootaxa
676 2220, 41–66.

677 Guayasamin JM, Krynak T, Krynak K, Culebras J, Hutter CR (2015). Phenotypic
678 plasticity raises questions for taxonomically important traits: A remarkable new
679 Andean rainfrog (Pristimantis) with the ability to change skin texture. Zoological
680 Journal of the Linnean Society, 173(4), 913–928. https://doi.org/10.1111/zoj.12222

681 Guayasamin JM, Hutter CR, Tapia EE, Culebras J, Peñafiel N, Pyron RA, Morochz
682 CW, Funk C, Arteaga A (2017) Diversification of the rainfrog *Pristimantis*
683 *ornatissimus* in the lowlands and Andean foothills of Ecuador. PLoS ONE 12:
684 e0172615. doi:10.1371/journal.pone.0172615

685 Hedges SB, Duellman WE, Heinicke MP (2008) New World direct-developing frogs
686 (Anura: Terrarana): Molecular phylogeny, classification, biogeography, and
687 conservation. Zootaxa, 1737, 1–182.

688 Heinicke MP, Duellman WE, Hedges SB (2007) Major Caribbean and Central
689 American frog faunas originated by ancient oceanic dispersal. Proceedings of the
690 National Academy of Sciences of the United States of America, 104, 10092–10097.

691 IUCN Standards and Petitions Subcommittee (2017) Guidelines for Using the IUCN
692 Red List Categories and Criteria. Version 13. Prepared by the Standards and Petitions
693 Subcommittee. http://www.iucnredlist.org/documents/RedListGuidelines.pdf.
694 [Accessed june 2019]

695 Jiménez de la Espada M (1875) Vertebrados del Viaje al Pacífico Verificado de 1862
696 a 1865 por una Comisión de Naturalistas Enviada por el Gobierno Español. Batracios.
697 Madrid: A. Miguel Ginesta.

698 Kalyaanamoorthy S, Minh BQ, Wong TK, von Haeseler A, Jermiin LS (2017)
699 ModelFinder: Fast model selection for accurate phylogenetic estimates. Nature
700 Methods, 14, 587–589. https://doi.org/10.1038/nmeth.4285

701 Köhler J, Jansen M, Rodríguez A, Kok PJR, Toledo LF, Emmrich M, Glaw F Haddad
702 CFB, Rödel M-O, Vences M (2017) The use of bioacoustics in anuran taxonomy:
703 theory, terminology, methods and recommendations for best practice. Zootaxa, 4251,
704 001–124.

705 Kumar S, Stecher G, Tamura K (2016) MEGA7: Molecular Evolutionary Genetics
706 Analysis version 7.0 for bigger datasets. Molecular Biology and Evolution 33:1870–
707 1874. https:// doi.org/10.1093/molbev/msw054

708 Lynch JD (1979) Leptodactylid frogs of the genus *Eleutherodactylus* from the Andes
709 of southern Ecuador. Miscellaneous Publication, Museum of Natural History,
710 University of Kansas 66, 1–62. https://doi.org/10.5962/bhl.title.16268

711 Lynch JD, Duellman WE (1980) The *Eleutherodactylus* of the Amazonian slopes of
712 the Ecuadorian Andes (Anura: Leptodactylidae). Miscelaneous Publication, Museum
713 of Natural History, University of Kansas 69, 1–86.
714 https://doi.org/10.5962/bhl.title.16222

715 Lynch JD, (1991) Three replacement names for preoccupied names in the genus
716 Eleutherodactylus (Amphibia: Leptodactylidae). Copeia 1991: 1138–1139.

717 Lynch JD, (1996) Replacement names for three homonyms in the genus
718 *Eleutherodactylus* (Anura: Leptodactylidae). Journal of Herpetology 30: 278–280.

719 Lynch JD, Duellman WE (1997) Frogs of the genus *Eleutherodactylus* in western
720 Ecuador: systematics, ecology, and biogeography. Special Publications, Natural
721 History Museum University of Kansas, 23, 1–236.
722 https://doi.org/10.5962/bhl.title.7951

723 Maddison WP, Maddison DR (2018) Mesquite: a modular system for evolutionary
724 analysis. Version 3.51. http://www.mesquiteproject.org [accessed 05 may 2019].

725 Mendoza AM, Ospina OE, Cárdenas-Henao H, García-R JC (2015) A likelihood
726 inference ofhistorical biogeography in the world's most diverse terrestrial vertebrate
727 genus: Diversification of direct-developing frogs (Craugastoridae: *Pristimantis*)
728 across the Neotropics. Molecular Phylogenetic Evolution, 85, 50–58.

729 Ministerio del Ambiente (2018) Cobertura de la tierra, Ecuador. Map.
730 http://ide.ambiente.gob.ec/mapainteractivo/ [accessed 15 april 2020].

731 Ministerio del Ambiente (2018) Deforestación periodo 2016 – 2018. Map.
732 http://ide.ambiente.gob.ec/mapainteractivo/ [accessed 15 april 2020].

733 Moen DS, Wiens JJ (2009) Phylogenetic evidence for competitively driven
734 divergence: body-size evolution in Caribbean treefrogs (Hylidae: *Osteopilus*).
735 Evolution 63, 195–214. EVO538 [pii]10.1111/j.1558-5646.2008.00538.x:

736 Mueses-Cisneros JJ (2005) Fauna anfibia del Valle de Sibundoy, Putumayo-
737 Colombia. Caldasia. Bogotá 27: 229–242.

738 Nguyen LT, Schmidt HA, von Haeseler A, Minh BQ (2015) IQ-TREE: A fast and
739 effective stochastic algorithm for estimating maximum likelihood phylogenies.
740 Molecular Biology and Evolution, 32, 268–274.
741 https://doi.org/10.1093/molbev/msu300

742 Ortega-Andrade HM, Rojas-Soto OR, Valencia JH, de los Monteros AE, Morrone JJ,
743 Ron SR, Cannatella DC (2015) Insights from integrative systematics reveal cryptic
744 diversity in *Pristimantis* frogs (Anura: Craugastoridae) from the Upper Amazon
745 Basin. PloS ONE 10: e0143392.

746 Ospina-Sarria JJ, Duellman WE (2019) Two new species of *Pristimantis* (Amphibia:
747 Anura: Strabomantidae) from southwestern Colombia. Herpetologica 75: 85–95

748 Padial JM, Grant T, Frost DR (2014) Molecular systematics of terraranas (Anura:
749 Brachycephaloidea) with an assessment of the effects of alignment and optimality
750 criteria. Zootaxa, 3825, 001–132.

751 Páez NB, Ron SR (2019) Systematics of *Huicundomantis*, a new subgenus of
752 *Pristimantis* (Anura, Strabomantidae) with extraordinary cryptic diversity and eleven
753 new species. Zookeys 868,1–112.

754 Restrepo A, Velasco JA, Daza JM (2017) Extinction risk or lack of sampling in a
755 threatened species: genetic structure and environmental suitability of the neotropical
756 frog *Pristimantis penelopus* (Anura: Craugastoridae). Papéis Avulsos de Zoologia, 57,
757 1-15. http://dx.doi.org/10.11606/0031-1049.2017.57.01.

758 Rivera-Correa M, Daza JM (2016). Molecular phylogenetics of the *Pristimantis*
759 *lacrimosus* species group (Anura: Craugastoridae) with the description of a new
760 species from Colombia. Acta Herpetologica, 11, 31–45.

761 Ron SR, Duellman WE, Caminer MA, Pazmiño D (2018) Advertisement calls and
762 DNA sequences reveal a new species of *Scinax* (Anura: Hylidae) on the Pacific

763 lowlands of Ecuador. PLoS ONE 13: e0203169. https://doi.org/10.1371/
764 journal.pone.0203169

765 Ron SR, Merino-Viteri A, Ortiz DA (2019) Anfibios del Ecuador. Version 2019.0.
766 Museo de Zoología, Pontificia Universidad Católica del Ecuador.
767 https://bioweb.bio/faunaweb/amphibiaweb, [accesed 5 may 2019]

768 Ron SR, Carrion J, Caminer MA, Sagredo Y, Navarrete MJ, Ortega JA, Varela AL,
769 Maldonado GA, Terán C. In press. Three new species of frogs of the genus
770 *Pristimantis* (Anura: Strabomantidae) with a redefinition of the *P. lacrimosus* species
771 group. Zootaxa.

772 Ryan MJ, Rand AS (1995) Female responses to ancestral advertisement calls in
773 Tungara frogs. Science 269: 390–392

774 Stuart SN, Hoffmann M, Chanson J, Cox N, Berridge R, Ramani P, Young B (2008)
775 Threatened Amphibians of the World. Barcelona, Spain; International Union for the
776 Conservation of Nature, Gland. Switzerland; Conservation International, Arlington,
777 Virginia, U.S.A.: Lynx Editions.

778 Vieites DR, Andreone F, Vences M, Köhler J, Wollenberg KC, Glaw F (2009). Vast
779 underestimation of Madagascar's biodiversity evidenced by an integrative amphibian
780 inventory. Proceedings of the National Academy of Sciences, 106, 8267–8272.

781 Wiens JJ, Fetzner JW, Parkinson CL, Reeder TW (2005) Hylid frog phylogeny and
782 sampling strategies for speciose clades. Systematic Biology, 54: 719–748.

783 Wiens JJ, Pyron RA, Moen DS (2011) Phylogenetic origins of local-scale diversity
784 patterns and the causes of Amazonian megadiversity. Ecology Letters 14, 643–652.
785 10.1111/j.1461-0248.2011.01625.x:

786 Wollenberg KC, Vieites DR, Van Der Meijden A, Glaw F, Cannatella DC, Vences M
787 (2008) Patterns of endemism and species richness in Malagasy cophyline frogs
788 support a key role of mountainous areas for speciation. Evolution 62: 1890–1907.
789 https://doi.org/10.1111/ j.1558-5646.2008.00420.x

790 **Table 1.** Genbank accession numbers for DNA sequences used for phylogenetic analyses.
791

Species	Voucher	12S	16S	RAG1	ND1
Niceforonia elassodisca	QCAZ 52495	Pending	Pending	Pending	Pending
Niceforonia nigrovittata	QCAZ 59410	NA	Pending	NA	NA
P. acerus	KU 217786	EF493678.1	EF493678.1	NA	NA
P. actites	KU 217830	NA	EF493696.1	EF493432.1	NA
P. aff. *subsigillatus*	QCAZ 58017	Pending	Pending	Pending	Pending
P. altamazonicus	KU 215460	EF493670.1	EF493670.1	NA	NA
P. amaguanae	QCAZ 39274	In press	In press	In press	In press
P. andinognomus	QCAZ 16683	NA	Pending	Pending	Pending
P. angustilineatus	UVC 15828	NA	JN371034.1	NA	NA
P. appendiculatus	KU177637	EF493524.1	EF493524.1	NA	NA
P. aureolineatus	QCAZ 42286	In press	In press	In press	NA
P. bambu	QCAZ 46708	NA	Pending	Pending	NA
P. boulengeri	MHUAA 8951	NA	KU724435.1	NA	NA
P. brevifrons	nrps 0059	JN991498.1	JN991433.1	NA	NA
P. bromeliaceus	QCAZ 16699	In press	In press	In press	In press
P. calcarulatus	KU 177658	EF493523.1	EF493523.1	NA	NA
P. cedros	MZUTI 1713	NA	KT210155.1	NA	NA
P. celator	QCAZ 66230	Pending	Pending	Pending	Pending
P. cf. *mendax*	MTD 45080	EU186659.1	EU186659.1	NA	NA
P. conspicillatus	QCAZ 28448	Pending	Pending	Pending	NA
	QCAZ 55439	NA	Pending	Pending	Pending
P. crucifer	KU 177733	EU186736.1	EU186718.1	NA	NA
P. curtipes	QCAZ 40722	Pending	Pending	Pending	Pending
P. degener	QCAZ 40304	Pending	Pending	Pending	Pending
P. diadematus	KU 221999	EU186668.1	EU186668.1	NA	NA
	QCAZ 59442	Pending	Pending	Pending	Pending
P. dissimulatus	KU179090	EF493522.1	EF493522.1	NA	NA
P. dorsopictus	MHUAA7638	KP082864.1	KP082874.1	NA	NA
P. ecuadorensis	CJ 5350	KX785339	KX785343	NA	KX785347
	CJ 5351	KX785340	KX785344	NA	KX785348
P. enigmaticus	QCAZ 40918	In press	In press	In press	In press
P. eremitus	QCAZ 40002	NA	NA	Pending	Pending
	QCAZ 49652	NA	Pending	Pending	Pending
	QCAZ 43392	NA	Pending	NA	NA
P. eugeniae	QCAZ 52367	Pending	Pending	Pending	Pending
P. galdi	QCAZ 32368	EU186670.1	EU186670.1	In press	NA
	QCAZ 58885	Pending	Pending	Pending	Pending
	QCAZ 58886	NA	Pending	Pending	NA
	QCAZ 58888	NA	Pending	Pending	NA
P. glandulosus	KU 218002	EF493676.1	EF493676.1	NA	NA

Species	Voucher	12S	16S	RAG1	ND1
P. imitatrix	KU 215476	EF493824.1	EF493667.1	NA	NA
P. inusitatus	KU 218015	EF493677.1	NA	NA	NA
P. jaguensis	MHUAA 7249	KP082862.1	KP082870.1	NA	NA
P. jorgevelosai	JDL 26123	NA	DQ195461.1	NA	NA
P. katoptroides	QCAZ 46360	NA	Pending	Pending	Pending
P. lacrimosus	QCAZ 55238	NA	In press	In press	In press
	QCAZ 59474	NA	In press	In press	NA
	QCAZ 40261	NA	In press	In press	In press
	QCAZ 59469	NA	In press	In press	NA
P. limoncochensis	QCAZ 43794	NA	In press	In press	In press
	QCAZ 19180	In press	In press	In press	NA
P. lymani	QCAZ 46311	NA	Pending	Pending	Na
P. melanogaster	NA	EF493826.1	EF493664.1	NA	NA
P. mindo	MZUTI 1382	NA	KF801584.1	NA	NA
	MZUTI 1381	NA	KF801583.1	NA	NA
	QCAZ 56512	NA	In press	In press	In press
	MZUTI 1756	NA	KF801581.1	NA	NA
	QCAZ 42197	In press	In press	In press	In press
P. moro	AJC 1860	JN991520.1	JN991454.1	JQ025191.1	NA
	AJC 1753	JN991519.1	JN991453.1	JQ025192.1	NA
P. muranunka	QCAZ 54593	NA	Pending	Pending	Pending
P. nankints	QCAZ 69137	NA	In press	In press	NA
P. nyctophylax	KU 177812	EF493526.1	EF493526.1	NA	NA
	QCAZ 32288	NA	In press	In press	In press
P. omeviridis	QCAZ 10564	In press	In press	In press	In press
	QCAZ 19664	NA	In press	In press	NA
P. orcesi	KU 218021	EF493679.1	EF493679.1	NA	NA
P. ornatissimus	MZUTI 4798	KU720464	KU720463	NA	KU720480
	MZUTI 4806	KX785337	KX785341	NA	KX785345
	MZUTI 4807	KX785338	KX785342	NA	KX785346
P. pahuma	MZUTI 493	NA	KT210158.1	NA	NA
P. petersi	QCAZ 63455	Pending	Pending	Pending	Pending
	QCAZ 63456	NA	Pending	Pending	Pending
P. petersioides	QCAZ 58936	NA	Pending	Pending	Pending
	QCAZ 58937	Pending	Pending	Pending	Pending
	QCAZ 58951	Pending	Pending	Pending	Pending
	QCAZ 58939	Pending	Pending	Pending	Pending
	QCAZ 59167	Pending	Pending	Pending	Pending
	QCAZ 58944	Pending	Pending	Pending	Pending
	QCAZ 59456	Pending	Pending	Pending	Pending
	QCAZ 59466	Pending	Pending	Pending	Pending
	QCAZ 59472	Pending	Pending	Pending	Pending

Species	Voucher	12S	16S	RAG1	ND1
	QCAZ 59479	Pending	Pending	Pending	Pending
	QCAZ 59625	Pending	Pending	Pending	Pending
	QCAZ 59470	Pending	Pending	Pending	Pending
	QCAZ 59471	Pending	Pending	Pending	Pending
	QCAZ 59468	Pending	Pending	Pending	Pending
	QCAZ 59458	Pending	Pending	Pending	Pending
	QCAZ 59461	Pending	Pending	Pending	Pending
P. platydactylus	MNCNDNA 5524	FJ438811.1	EU192255.1	NA	NA
P. pulvinatus	KU 181015	EF186741.1	EF186723.1	NA	NA
P. pycnodermis	KU 218028	EF493680.1	EF493680.1	NA	NA
P. quaquaversus	QCAZ 25613	Pending	Pending	Pending	Pending
P. romeroae	QCAZ 41121	In press	In press	In press	In press
P. roni	QCAZ 58897	NA	Pending	NA	NA
P. rubicundus	QCAZ 58932	NA	In press	In press	NA
	QCAZ 58932	NA	Pending	Pending	NA
P. schultei	KU 212220	EF493681.1	EF493681.1	NA	NA
P. sp. 1	KU 291702	EF493351.1	EF493351.1	NA	NA
P. sp. *2*	QCAZ 63481	NA	Pending	NA	Pending
	QCAZ 63482	NA	Pending	Pending	Pending
P. sp. UCS1	QCAZ 60398	NA	In press	In press	NA
P. sp. UCS2	QCAZ 62940	In press	In press	NA	In press
P. sp. UCS3	QCAZ 58956	In press	In press	In press	NA
P. subsigillatus	MECN 10117	NA	KF801580.1	NA	NA
	QCAZ 45268	NA	Pending	Pending	Pending
	QCAZ 49370	Pending	Pending	Pending	Pending
	QCAZ 51314	NA	Pending	Pending	Pending
	QCAZ 50012	NA	Pending	Pending	Pending
	KU 218147	EF493525.1	EF493525.1	NA	NA
	QCAZ 49637	NA	In press	In press	In press
P. truebae	QCAZ 13752	NA	Pending	Pending	Pending
	QCAZ 42714	Pending	Pending	Pending	Pending
P. urani	MHUAA 7471	NA	KU724442.1	NA	NA
P. w-nigrum	QCAZ 45200	In press	In press	In press	In press
	QCAZ 46256	NA	In press	In press	In press
	QCAZ 41818	NA	In press	NA	In press
	QCAZ 52365	NA	Pending	Pending	Pending
P. zeuctotylus	ROM 43978	EU186678.1	EU186678.1	NA	NA

792
793 **Table 2.** Character loadings, eigenvalues, and percentage of explained variance for Principal
794 Components (PC) I–II. The analysis was based on morphological variables of adults of *P.*
795 *petersioides* sp. nov. and *P. petersi.* Bold figures indicate highest loadings.
796

Variable	Character Loading	
	PC I	PC II
Tibia length	**0.7855**	-0.3038
Foot length	0.7066	0.0834
Head length	**0.7873**	0.2181
Head width	**0.8332**	0.2434
Tympanum	-0.2087	**0.9334**
Eigenvalues	4.9483	2.1547
%	49.48	21.54

797

798 **Table 3.** Quantitative and qualitative characteristics of the advertisement call of *Pristimantis petersioides* sp. nov. from two localities:
799 Sardinayacu, Morona Santiago Province (2.0983° S, 78.1155° W, 1345 m a.s.l.) and Yurugyacu river, Llanganates National Park, Pastaza
800 Province, Ecuador (1.3524º S, 78.0597º W, 1419 m a.s.l.) in comparison with *Pristimantis petersi* from Cocodrilos, Napo Province (0.6710° S,
801 77.7927° W, 1575 m a.s.l.). Mean is given with range in parentheses
802

	Pristimantis petersioides QCAZ 58940	*Pristimantis petersioides* QCAZ 59466	*Pristimantis petersioides* (not collected)	*Pristimantis petersi* (not collected)	*Pristimantis petersi* (not collected)
Calls analyzed	47	37	13	4	9
Call duration (s)	0.19 (0.11–0.32)	0.32 (0.16–0.39)	0.25 (0.19–0.34)	0.46 (0.41–0.49)	0.37(0.31–0.44)
Call rate (calls/minute)	11.26 (1.77–18.40)	25.78 (4.52–35.14)	22.64 (12–17.88)	4.24 (1.86–6.62)	9.04 (2.17–33.18)
Call interval (s)	6.21 (3.03–33.66)	2.49 (1.37–13.09)	2.44 (1.82–3.05)	20.16 (8.59–31.73)	11.13(1.41–27.20)
Call rise time (s)	0.03 (0.021–0.036)	0.013 (0.011–0.019)	0.008 (0.004–0.015)	0.064(0.04–0.12)	0.0107(0.07–0.18)
Notes per call	1	1	1	1	1
Number of harmonics	3	4	1	1	1
Fundamental frequency (Hz)	4837.22 (4373.4–5092.6)	4122 (3644.5–4382.8)	4333.1 (4295.9–4392.8)	3846.7(3820.3–3890.6)	4076.8 (3914.1–4242.2)
Dominant frequency (Hz)	4837.2 (4373.4–5092.6) (1st harmonic)	4122 (3644.5–4382.8) (1st harmonic)	4333.1 (4295.9–4392.8) (1st harmonic)	3846.7(3820.3–3890.6) (1st harmonic)	4076.8 (3914.1–4242.2) (1st harmonic)

803

804 **Table 4.** Qualitative morphological characters of species most similar to *P. petersioides* sp. nov.
805

	Maximun size in females	Eyelid tubercle	Discoidal fold	Dorsal snout shape	Lateral snout shape	TY/ED	Knee tubercle	Heel tubercle	Dorsum	Data source
P. bromeliaceus	27.20 mm	2-3 non conical	prominent	subacuminate	pointed	1/4 to 2/5	small wart	conical	smooth	Lynch , 1979
P. lacrimosus	32.5 mm	absent	evident	rounded	rounded	3/10	absent	absent	finely shagreen	Jimenez de la Espada, 1875
P. petersi	21.11 mm	conical	absent	rounded	truncate	3/5 to 1/2	absent	absent	smooth	Herein
P. petersioides	24.81 mm	conical	ill-defined	rounded to truncate	truncate	2/5 to 1/2	absent	absent	smooth to shagreen	Herein
P. rhodostichus	29.50 mm	several low	prominent	long, acuminate	acutely rounded	2/5	absent	absent	finely shagreen	Duellman and Pramuk, 1999
P. schultei	34.00 mm	several low	not evident	acuminate	inclined posteroventrally	2/5 to 1/2	absent	several low	shagreen	Duellman, 1990

806
807

808 **Table 5**. Morphometric variables of *P. petersioides* sp. nov. and *P. petersi.* Mean ± SD is given with
809 range in parentheses. All measurements are in millimeters.

810

	P. petersioides **sp. nov**.		*P. petersi*	
	male	female	male	female
Variable	n = 39	n = 15	n = 10	n = 2
Snout-vent length	18.53 ± 1.52 (15.79–23.93)	22.80 ± 1.37 (20.42–24.81)	18.33 ± 1.71 (16.49 –22.65)	20.11 ± 1.42 (19.11–21.11)
Tibia length	9.81 ± 0.78 (8.32–11.88)	11.74 ± 1.01 (8.48–12.57)	9.64 ± 0.62 (8.59–10.96)	10.70 ± 1.61 (9.56–11.84)
Foot length	8.64 ± 0.92 (6,94–10.65)	10.60 ± 0.71 (8.83–11.62)	8.62 ± 0.70 (7.78–10.07)	9.98 ± 0.28 (9.78–10.18)
Head length	6.50 ± 0.57 (5.34–7.80)	7.98 ± 0.57 (7.20–9.11)	6.10 ± 0.51 (5.52–7.06)	7.14 ± 0.49 (6.79–7.48)
Head width	6.96 ± 0.62 (5.90–8.50)	8.79 ± 0.46 (7.99–9.45)	6.93 ± 0.53 (6.28–8.07)	7.73 ± 0.39 (7.45–8.00)
Eye diameter	2.59 ± 0.23 (2.15–3.05)	2.99 ± 0.32 (2.42–3.52)	2.64 ± 0.24 (2.38–3.12)	2.79 ± 0.03 (2.76–2.82)
Tympanum diameter	0.91 ± 0.11 (0.69–1.06)	1.13 ± 0.15 (0.82–1.38)	0.90 ± 0.08 (0.73–1.02)	1.07 ± 0.17 (0.95–1.20)
Interorbital distance	2.23 ± 0.19 (1.89–2.57)	2.64 ± 0.17 (2.39–2.99)	2.18 ± 0.12 (2.02–2.45)	2.57 ± 0.19 (2.44–2.70)
Upper eyelid width	2.15 ± 0.25 (1.57–2.59)	2.63 ± 0.19 (2.33–2.95)	2.08 ± 0.37 (1.72–2.90)	2.27
Internarial distance	1.40 ± 0.10 (1.23–1.65)	1.71 ± 0.13 (1.51–2.00)	1.48 ± 0.15 (1.30–1.73)	1.58 ± 0.21 (1.43–1.72)
eye–nostril distance	1.94 ± 0.20 (1.59–2.48)	2.45 ± 0.19 (2.16–2.76)	2.06 ± 0.33 (1.82–2.93)	2.32 ± 0.37 (2.07–2.58)

811

Figures

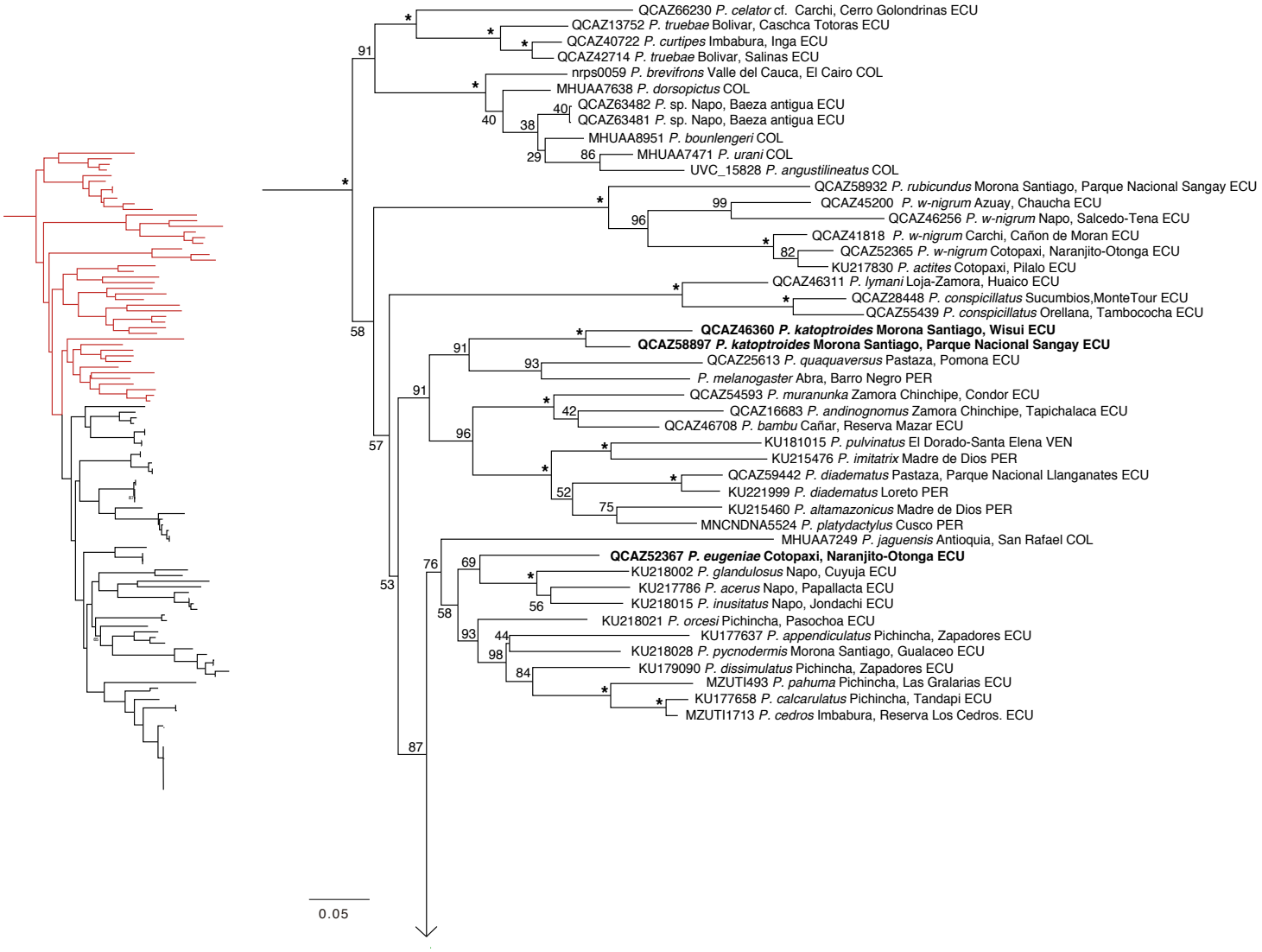

Figure 1. Maximum likelihood tree of the *Pristimantis lacrimosus* group inferred from a partitioned analysis of 4021 aligned sites of DNA sequences of genes 12S, 16S, ND-1 and RAG-1. Bold characters highlight species included for the first time in a phylogeny, red taxa highlight previously misidentified species. *Pristimantis petersioides* sp. nov. is highlighted in purple and the unconfirmed candidate species (UCS) are also colored, P. sp. UCS1 (pink), P. sp. UCS2 (blue), P. sp. UCS3 (green). Non-parametric bootstrap support values are shown on branches (asterisks denote 100 values). The outgroup was composed on specimens of *Niceforonia* (not shown). Number for voucher museum specimens are shown to the left of the species name; locality is shown to the right and country abbreviation at the end. Abbreviations: **ECU** Ecuador, **PER** Peru, **COL** Colombia, **VEN** Venezuela, **GUY** Guyana, **PAN** Panama.

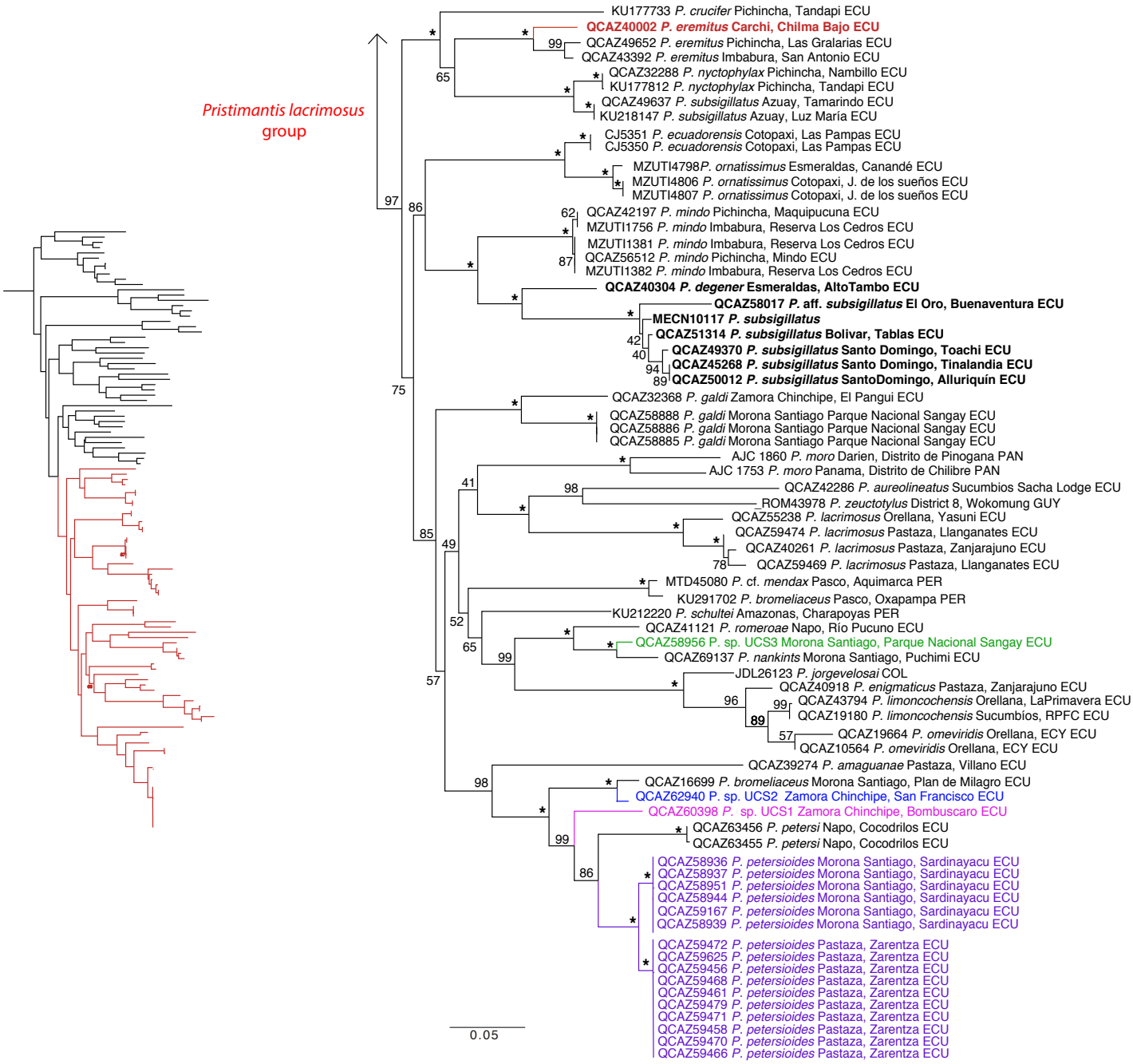

825

826 **Figure 1. Continued.**

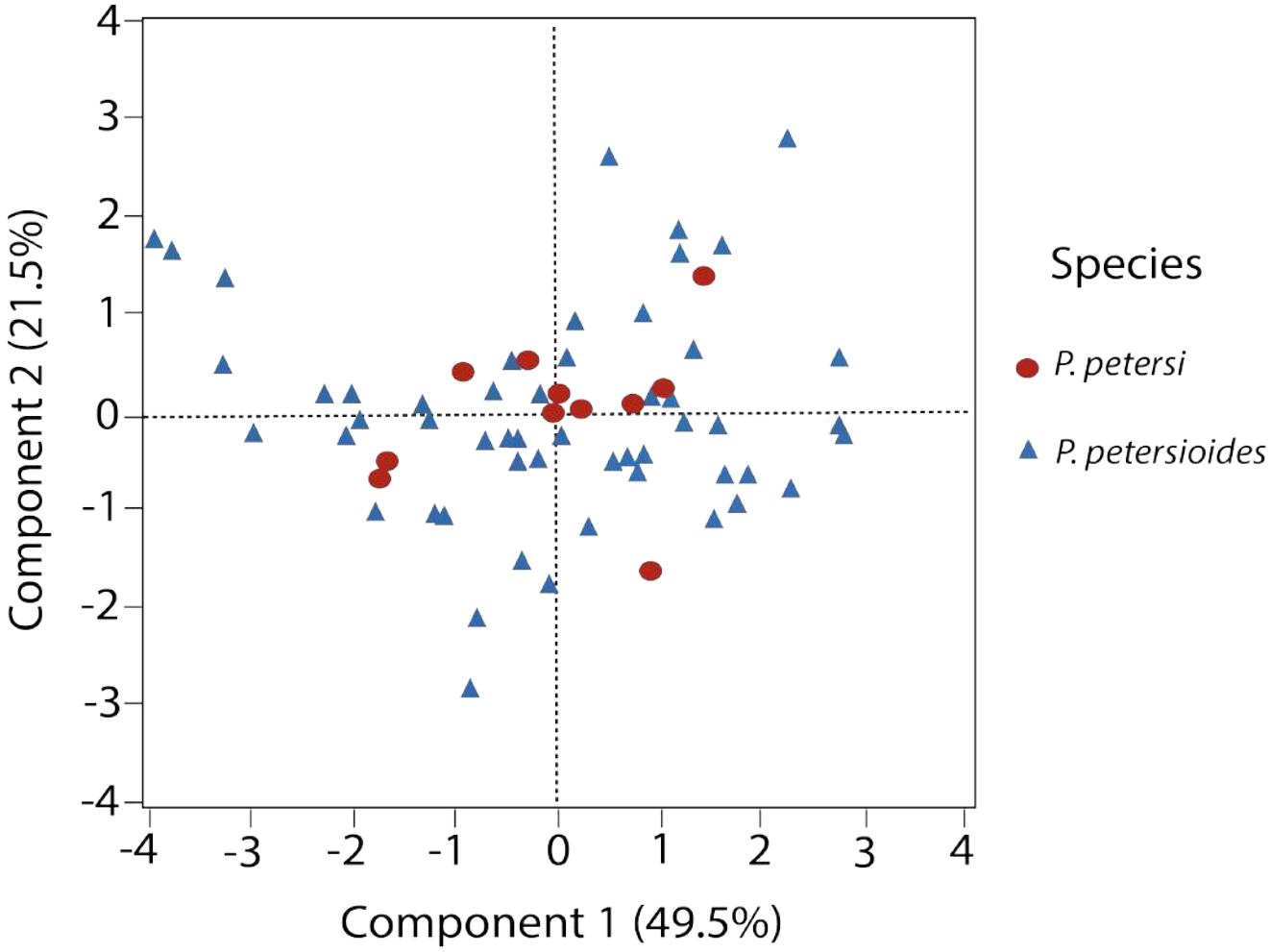

827

828 **Figure 2.** Principal components 1 and 2 from analysis of five size-corrected morphological
829 variables. See Table 2 for character loadings on each component.

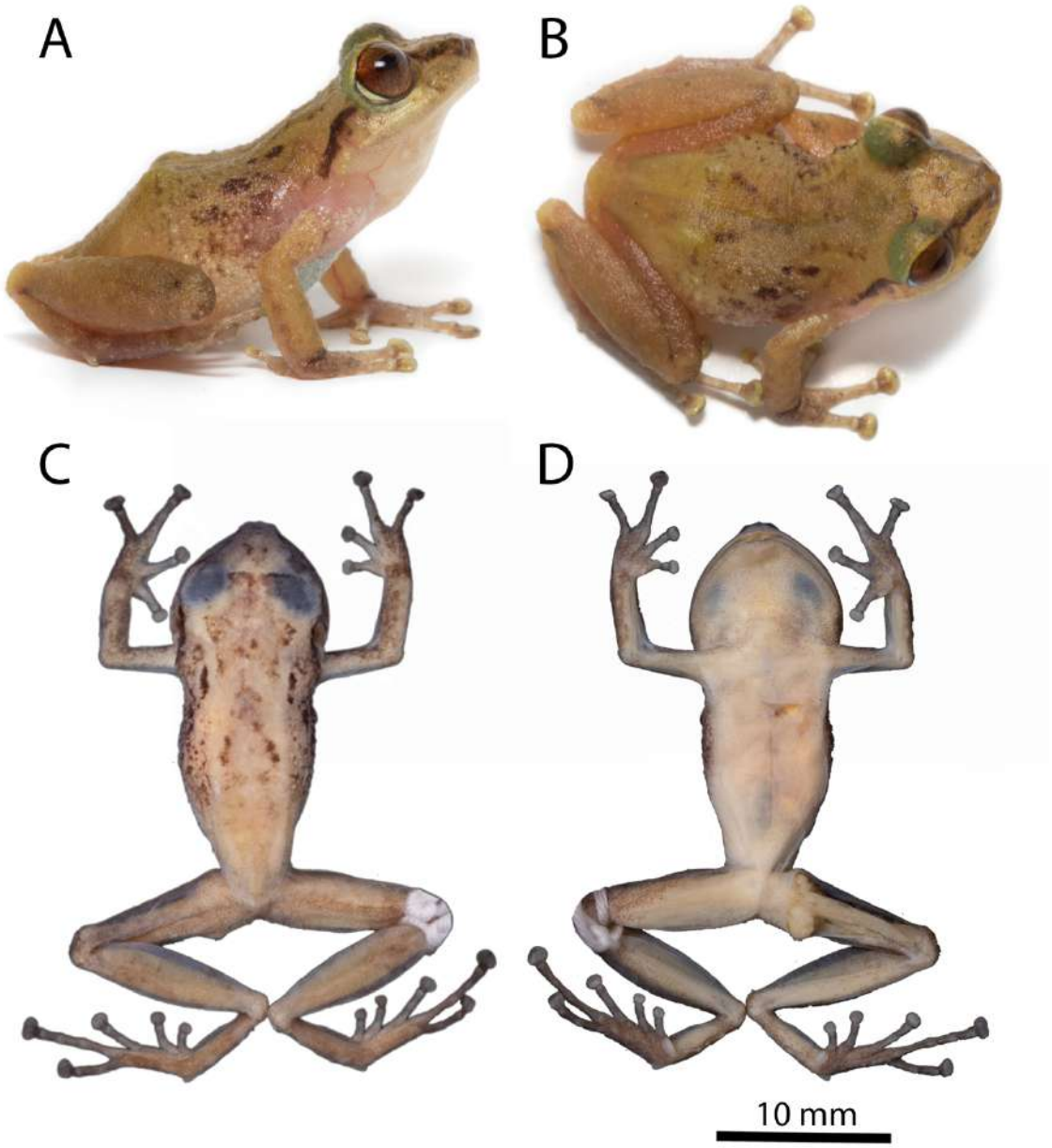

Figure 3. Holotype of *Pristimantis petersioides* sp. nov. QCAZ 58939, adult female, SVL = 22.02 mm. Sangay National Park, Sardinayacu, Ecuador. **A** lateral view of live individual, **B** dorsal view of live individual, **C** dorsal view of preserved individual, **D** ventral view of preserved individual. Photographs **A–B** by Juan Carlos Sánchez, **C–D** by Julio C. Carrión-Olmedo

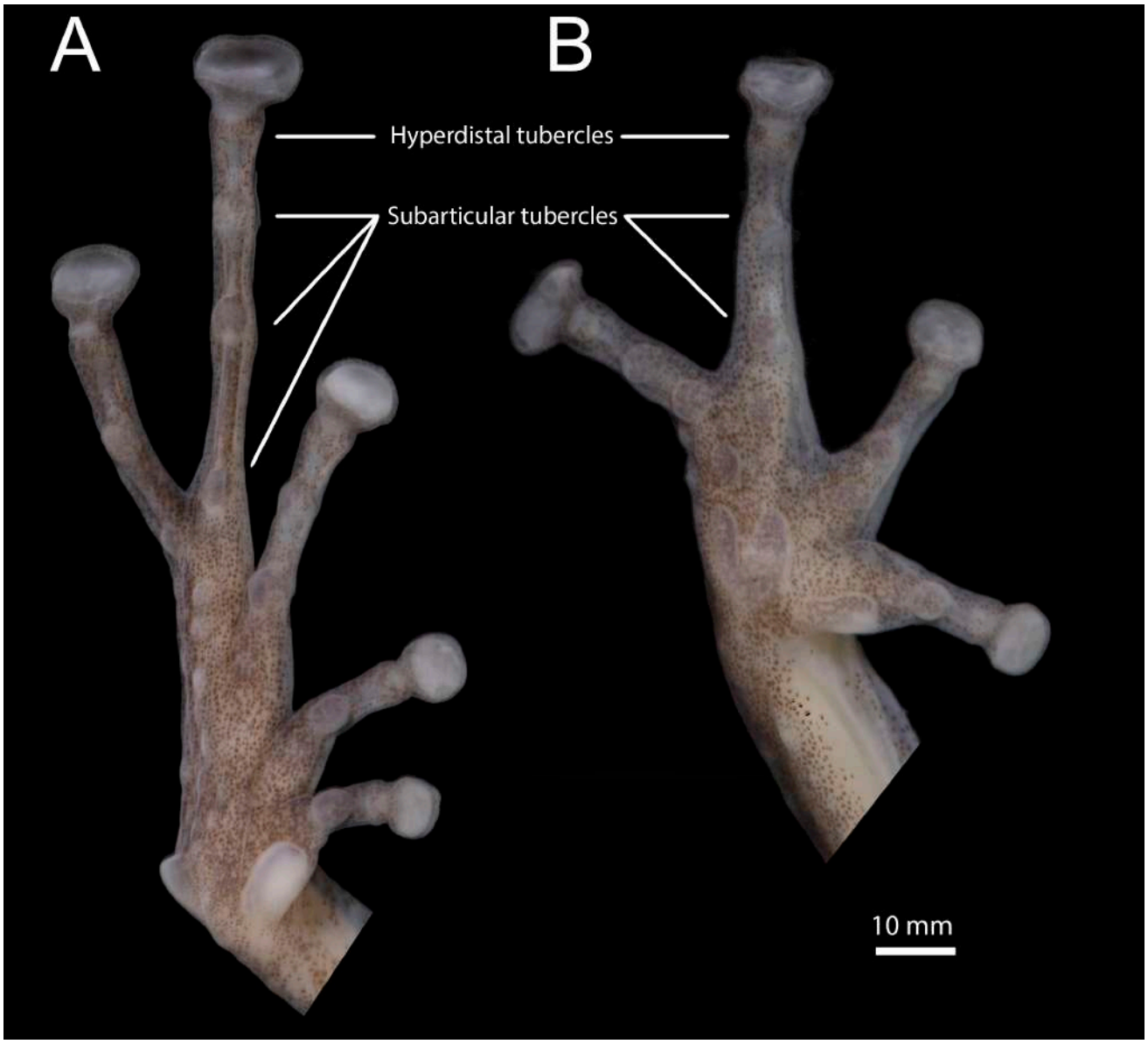

835

836 **Figure 4.** Hand and foot of the holotype of *Pristimantis petersioides* sp. nov. Ventral views of
837 right foot **A** and right hand **B**. Sangay National Park, Sardinayacu, Ecuador, SVL = 22.02 mm.
838 QCAZ 58939, adult female. Photographs by Julio C. Carrión-Olmedo.

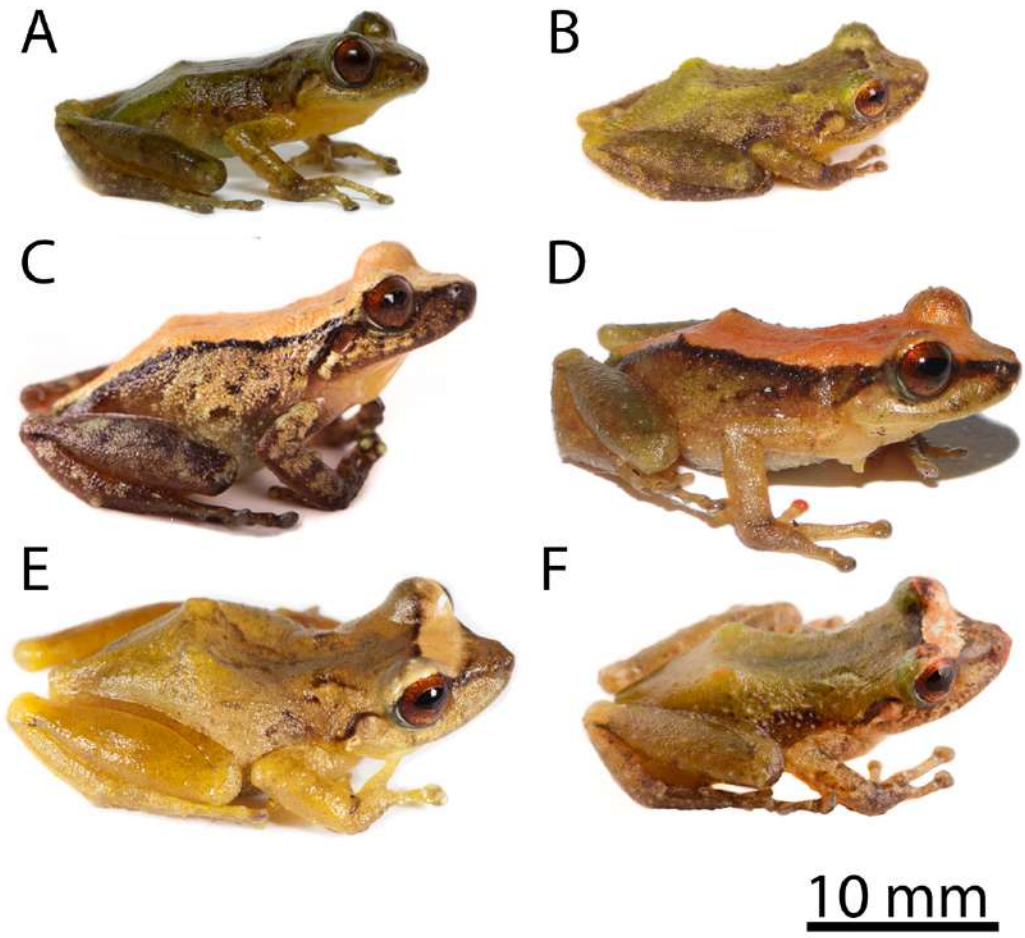

839

840 **Figure 5.** Live specimens of *Pristimantis petersioides* sp. nov. and most similar species. **A**
841 *Pristimantis petersioides*, QCAZ 63455, adult male (SVL 17.99 mm), **B** *Pristimantis petersi,*
842 QCAZ59455, adult male (SVL 16.49 mm), **C** *Pristimantis* sp. UCS2, QCAZ 62940, adult male (SVL
843 23.45 mm), **D** *Pristimantis bromeliaceus,* QCAZ 56454, adult male (SVL 21.93 mm) **E** *Pristimantis*
844 *schultei,* QCAZ 51551, adult male (SVL 24.60 mm), **F** *Pristimantis rhodostichus,* QCAZ 49027
845 (SVL 20.35 mm). Photographs by Juan Carlos Sánchez **A**, by David Velalcázar **B**, by Valeria
846 Chasiluisa **C**, by Jorge Brito **D**, by Diego Paucar **E**, by Santiago R. Ron **F**.

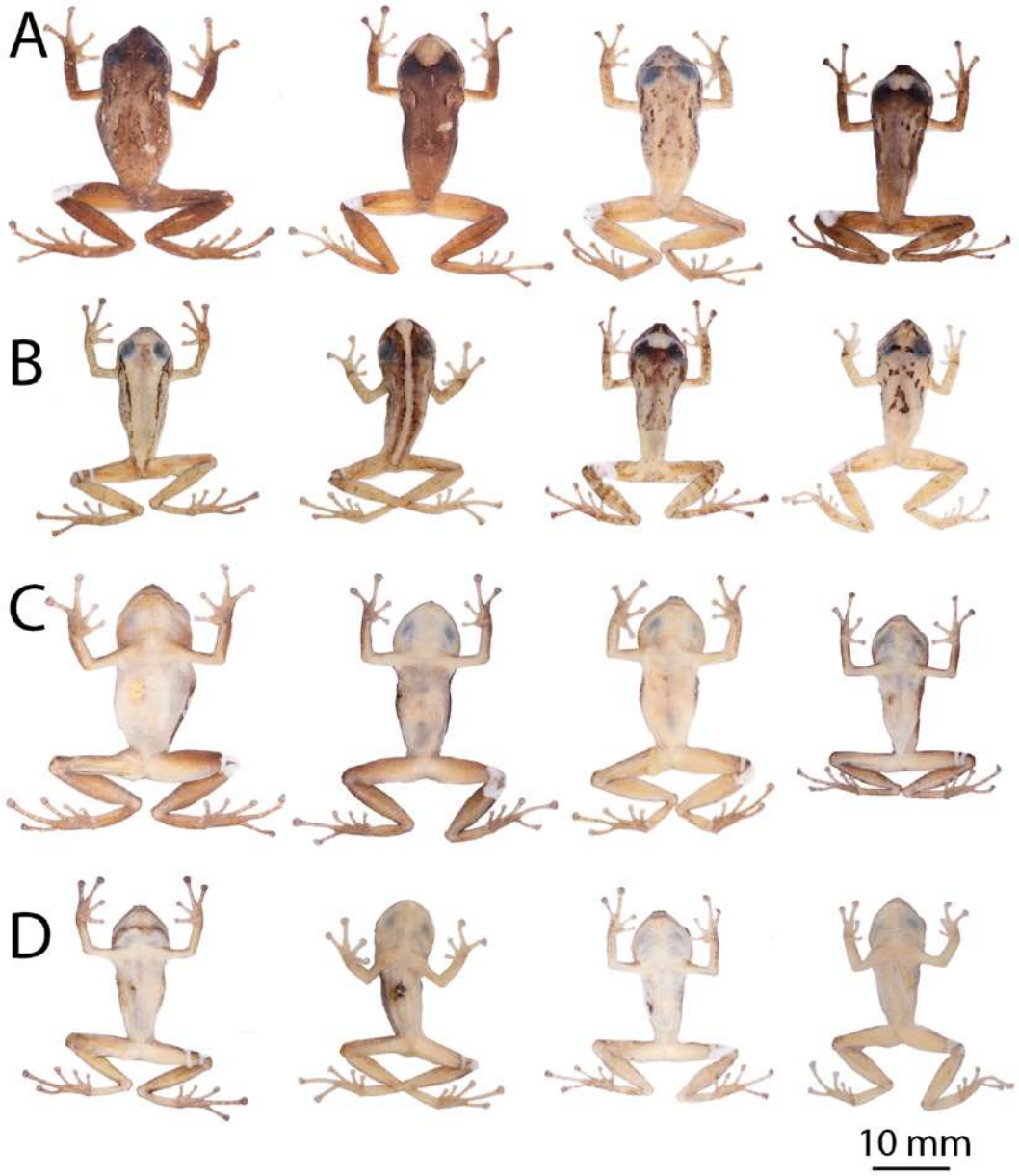

847

848 **Figure 6.** Color variation in preserved individuals of *Pristimantis petersioides* sp. nov. **A**
849 Dorsal view (left to right): QCAZ 59461(SVL 22.95 mm), QCAZ 59470 (SVL 22.94 mm), QCAZ
850 58939 (SVL 22.02 mm), QCAZ 58951 (SVL 19.75 mm), **B** Dorsal view (left to right): QCAZ 59171
851 (SVL 19.50 mm), QCAZ 59456 (SVL 19.05 mm), QCAZ 59462 (SVL 19.00 mm), QCAZ 59468
852 (SVL 18,35 mm), **C** Ventral view of specimens in (**A**), **D** Ventral view of specimens in (**B**).
853 Photographs by Julio C. Carrión-Olmedo.

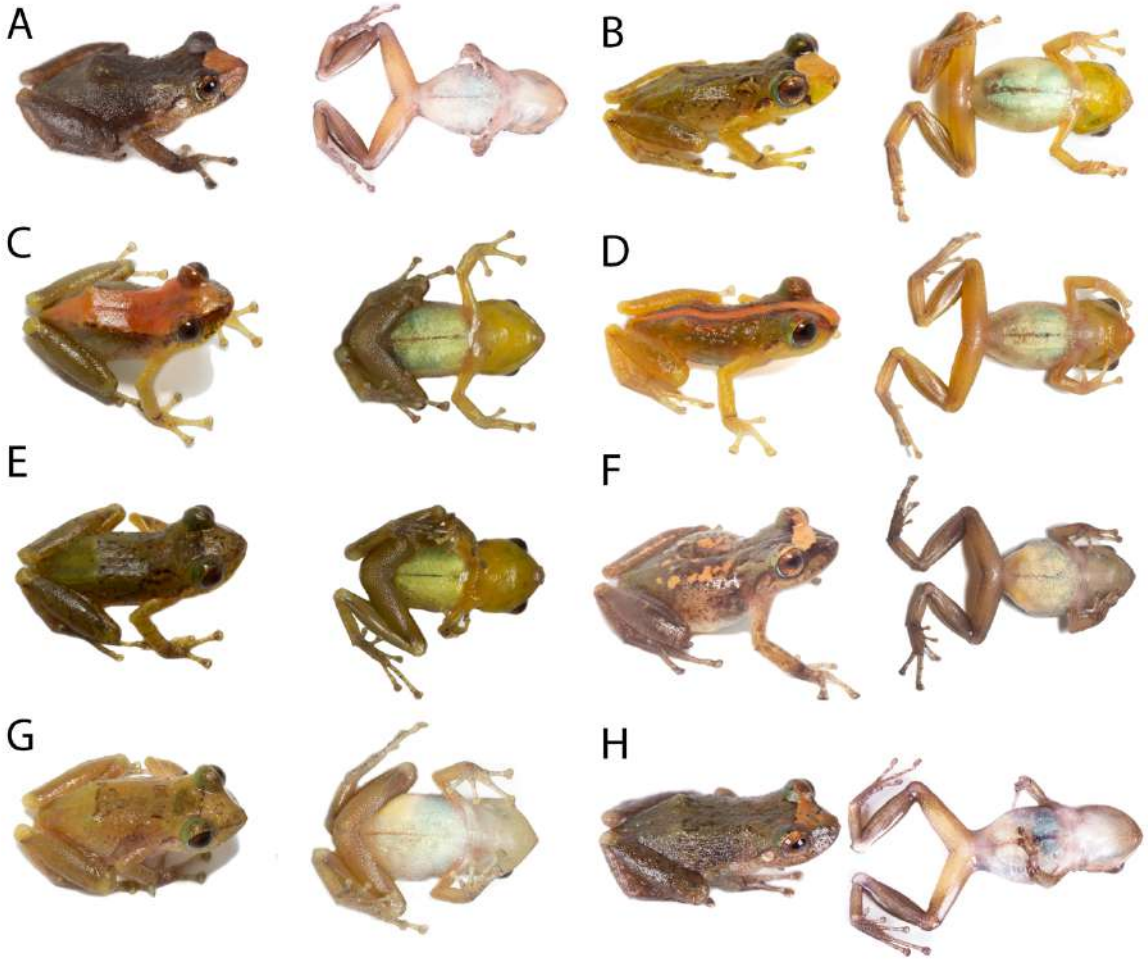

854

855 **Figure 7.** Variation in live adult individuals of *Pristimantis petersioides* sp. nov. **A** QCAZ
856 59471(SVL 17.45 mm), **B** QCAZ 59455 (SVL 18.2 mm), **C** QCAZ 58943 (SVL 17.73 mm), **D**
857 QCAZ 59456 (SVL 19.05 mm), **E** QCAZ 58938 (SVL 17.99 mm), **F** QCAZ 59458 (SVL 21.84
858 mm), **G** QCAZ 58941 (SVL 20.42 mm), **H** QCAZ 59466 (SVL 19.06 mm). Dorsolateral view on the
859 left, ventral view on the right. Photographs **A** and **H** by Santiago R. Ron, **B–G** by Juan Carlos
860 Sánchez.

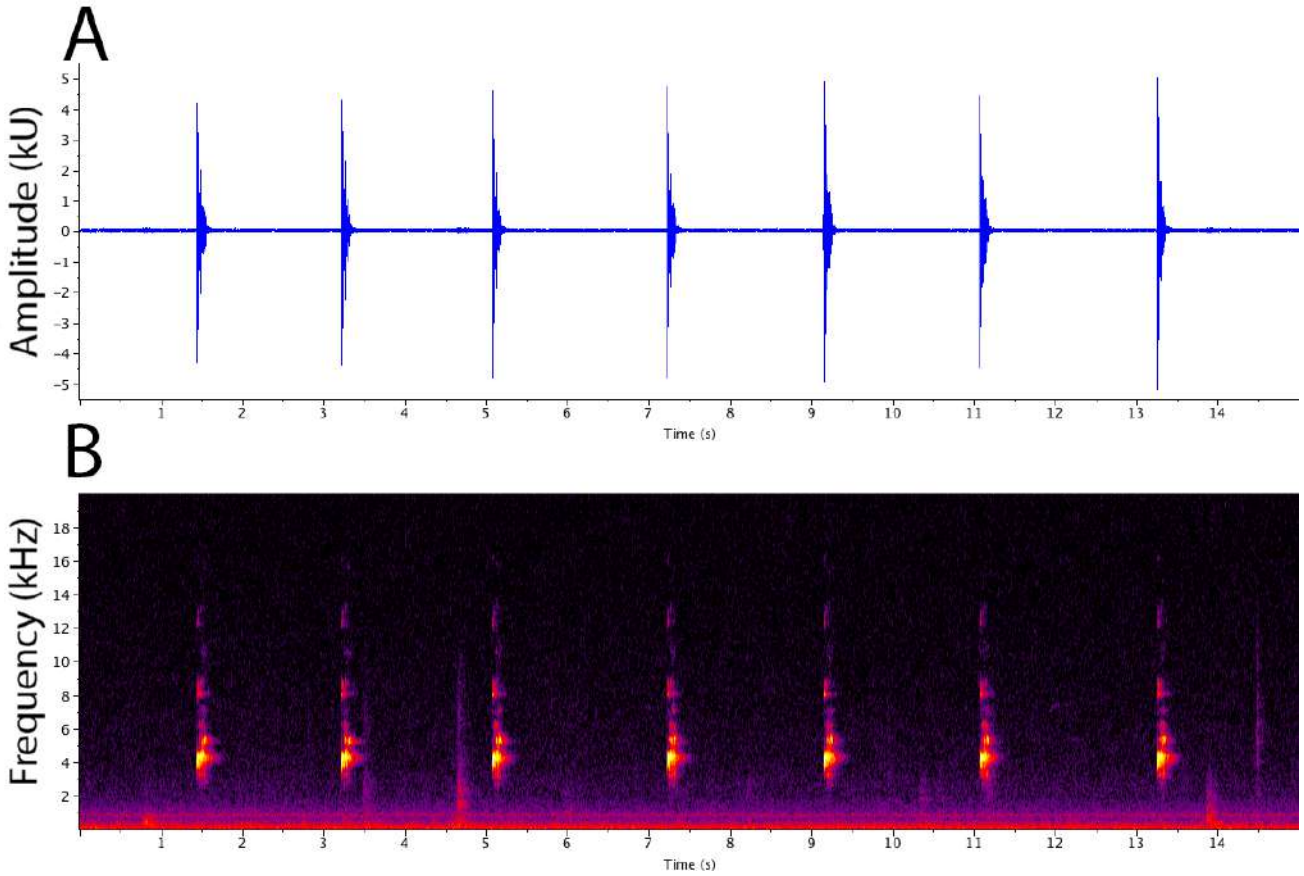

Figure 8. Oscillogram (A) and spectrogram (B) of a call series of *Pristimantis petersioides* sp. nov.

865

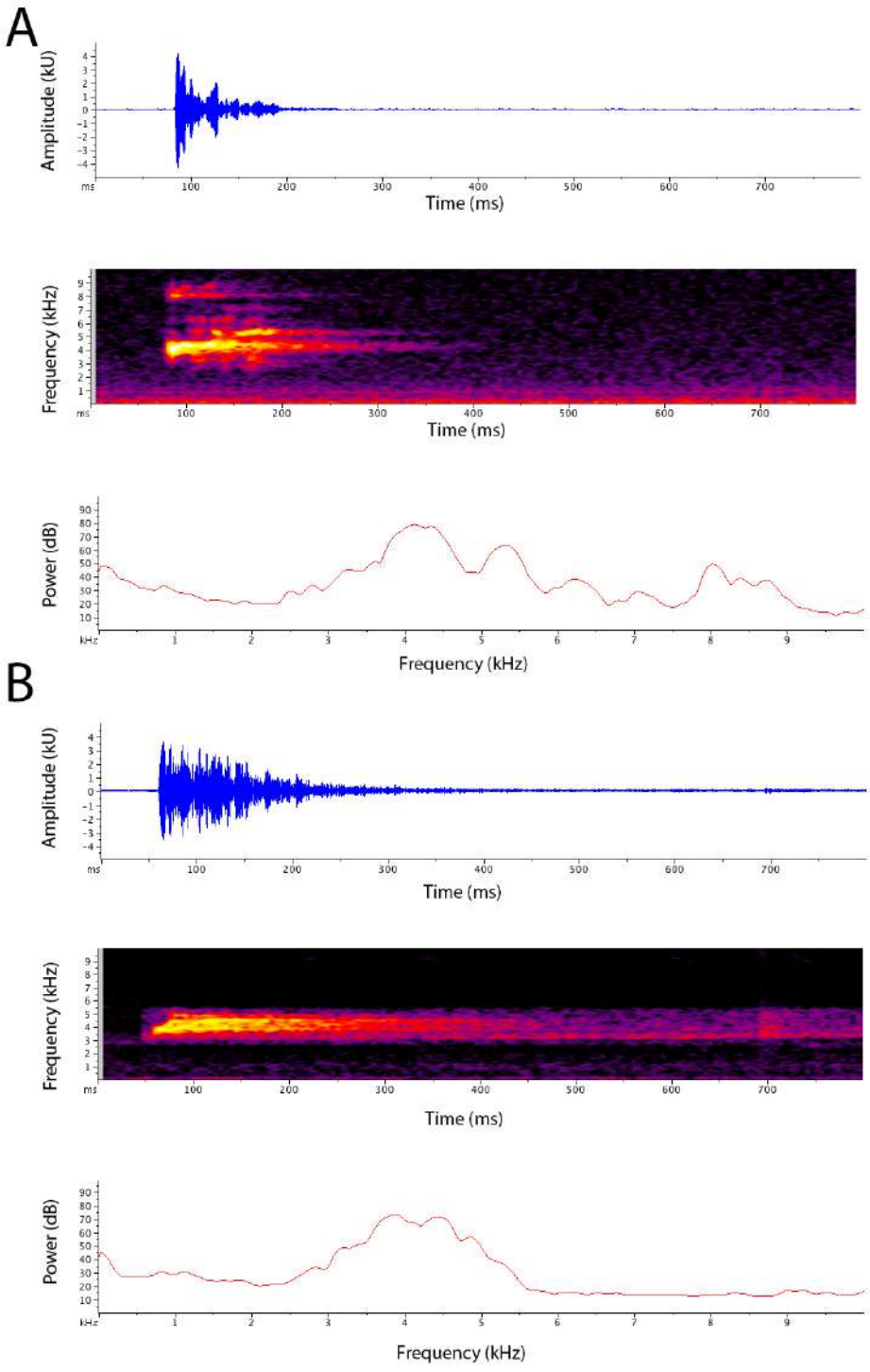

866

867 **Figure 9.** Advertisement calls of *Pristimantis petersioides* sp. nov. (A) and *Pristimantis petersi*
868 (B) showing oscillogram (top), sound spectrogram (middle), and power spectrum (bottom).

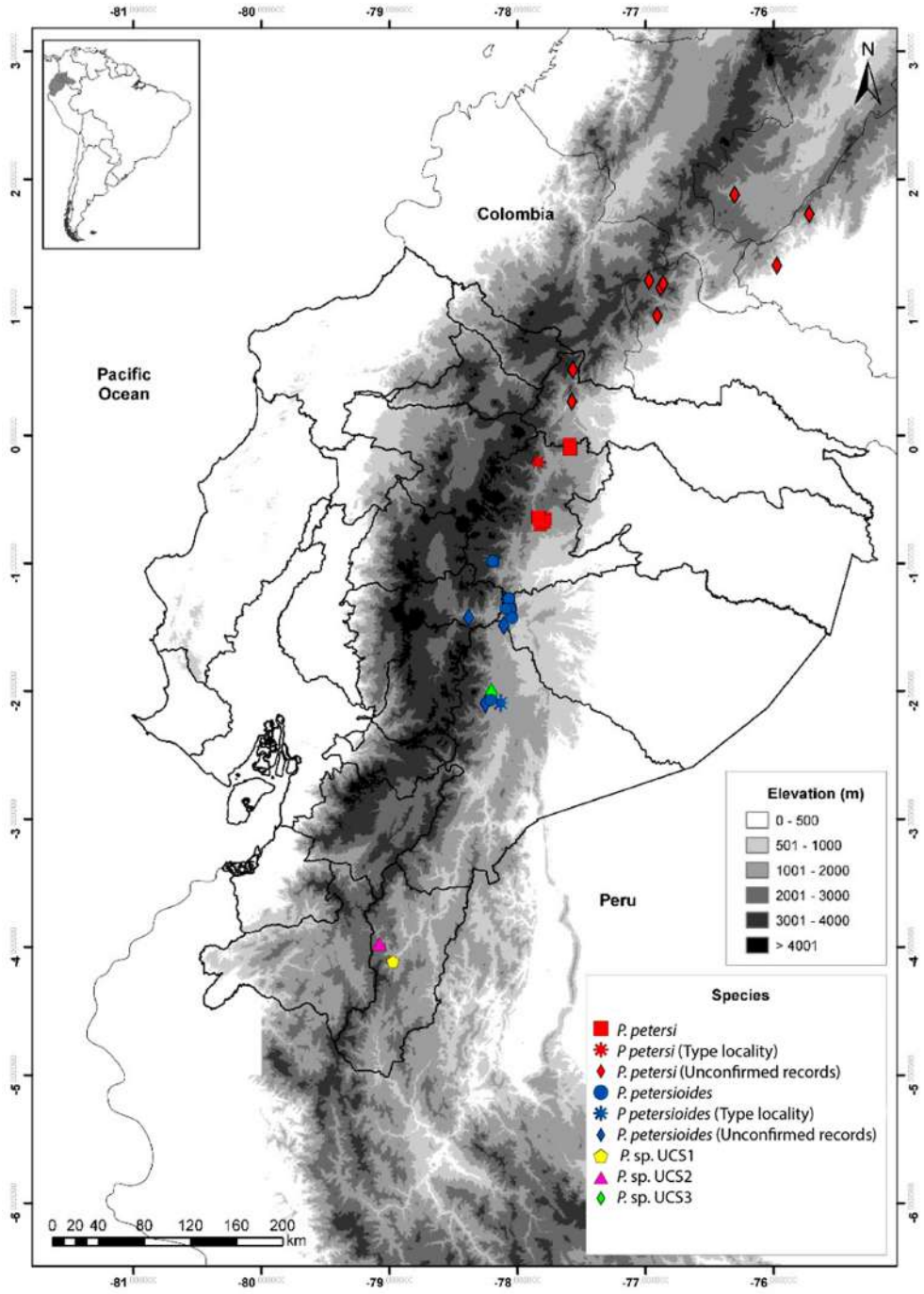

Figure 10. Records of *Pristimantis petersioides* sp. nov. (blue circles) and type locality (blue star) based on specimens deposited at the Museum of Zoology, Pontificia Universidad Católica del Ecuador, and unconfirmed records (blue diamond) from Lynch and Duellman (1980) and Brito et al. 2017. Confirmed records of *Pristimantis petersi* (red squares) based on specimens deposited at the Museum of Zoology, Pontificia Universidad Católica del Ecuador, type locality (red star) inferred by written description from Lynch and Duellman (1980) and unconfirmed records (red diamonds) inferred by written description from Lynch and Duellman (1980), records of Mueses-Cisneros (2005) and map from Stuart et al. (2008).

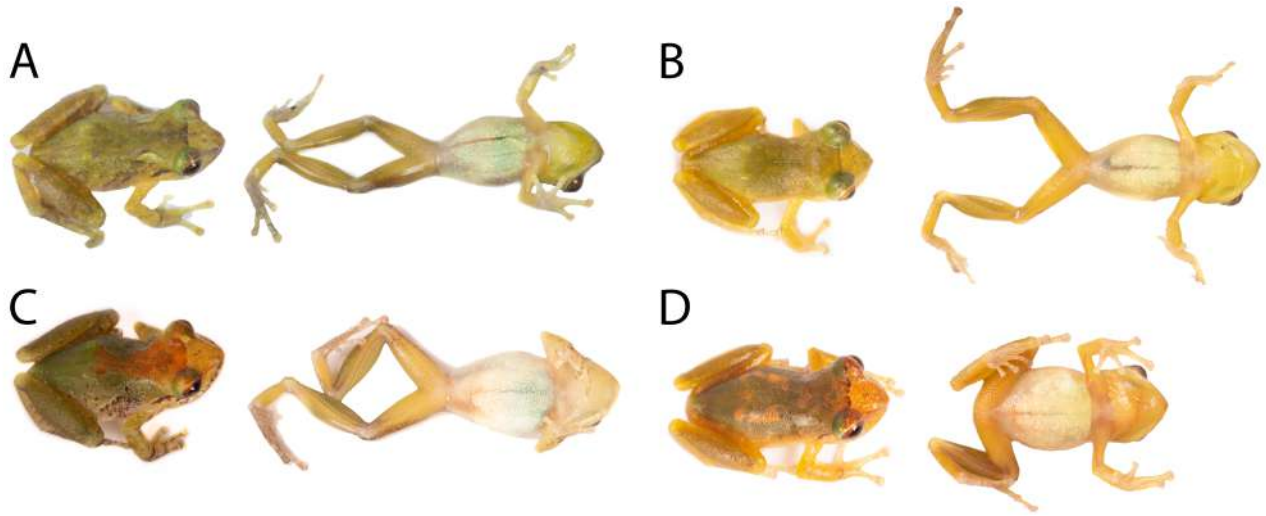

878

879 **Figure 11.** Variation in live adult individuals of *Pristimantis petersi*. **A** QCAZ 63452 (SVL 17.42
880 mm), **B** QCAZ 63453 (SVL 17.75 mm), **C** QCAZ 63454 (SVL 21.11 mm), **D** QCAZ 63456 (SVL
881 19.11 mm). Photographs by Santiago R. Ron **A**, by David Velalcázar **B–D**.